J|A|C|S
ARTICLES
Published on Web 06/06/2006

Nonchelated d^0 Zirconium−Alkoxide−Alkene Complexes

Edward J. Stoebenau, III and Richard F. Jordan*

Contribution from the Department of Chemistry, The University of Chicago, 5735 South Ellis Avenue, Chicago, Illinois 60637

Received November 3, 2005; Revised Manuscript Received April 26, 2006; E-mail: rfjordan@uchicago.edu

Abstract: The reaction of $Cp'_2Zr(O^tBu)Me$ ($Cp' = C_5H_4Me$) and $[Ph_3C][B(C_6F_5)_4]$ yields the base-free complex $[Cp'_2Zr(O^tBu)][B(C_6F_5)_4]$ (**6**), which exists as $Cp'_2Zr(O^tBu)(ClR)^+$ halocarbon adducts in CD_2Cl_2 or C_6D_5Cl solution. Addition of alkenes to **6** in CD_2Cl_2 solution at low temperature gives equilibrium mixtures of $Cp'_2Zr(O^tBu)(alkene)^+$ (**12a**−**l**), **6**, and free alkene. The NMR data for **12a**−**l** are consistent with unsymmetrical alkene bonding and polarization of the alkene C=C bond with positive charge buildup at C_{int} and negative charge buildup at C_{term}. These features arise due to the lack of d−π* back-bonding. Equilibrium constants for alkene coordination to **6** in CD_2Cl_2 at −89 °C, $K_{eq} = [\mathbf{12}][\mathbf{6}]^{-1}[alkene]^{-1}$, vary in the order: vinylferrocene (4800 M^{-1}) ≫ ethylene (7.0) ≈ α-olefins > *cis*-2-butene (2.2) > *trans*-2-butene (<0.1). Alkene coordination is inhibited by sterically bulky substituents on the alkene but is greatly enhanced by electron-donating groups and the β-Si effect. Compounds **12a**−**l** undergo two dynamic processes: reversible alkene decomplexation via associative substitution of a CD_2Cl_2 molecule, and rapid rotation of the alkene around the metal−(alkene centroid) axis.

Introduction

Zirconocene-catalyzed polymerization of alkenes is an industrially important reaction that enables the efficient synthesis of polyolefins with exquisite and predictable control of polymer structure.[1] Chain growth in this process occurs by coordination of an alkene to a d^0 Cp_2ZrR^+ metal−alkyl species, followed by insertion into the metal−alkyl bond,[2] as shown in Scheme 1. The intermediate $Cp_2Zr(R)(alkene)^+$ species have not been detected, and computational studies predict that the alkene insertion step has a low barrier or is near barrierless.[3,4] Analogous d^0 metal−hydride−alkene species are likely intermediates in β-H elimination, an important chain transfer process (Scheme 1). Studies of model d^0 metal−alkene complexes may provide insight into many features of polymerization processes, including catalyst structure/performance relationships, insertion regiochemistry, tacticity control, and monomer reactivity trends in copolymerization.

The Dewar−Chatt model of d^n metal−alkene bonding ($n \geq 2$) comprises two components: σ-donation from the alkene π orbital to a metal-acceptor orbital, and π-back-bonding from a metal d orbital to the alkene π* orbital (Figure 1).[5] The d−π* back-bonding strengthens the metal−alkene interaction and

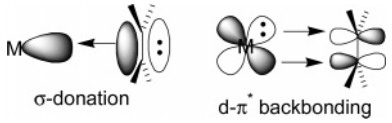

Figure 1. Dewar−Chatt model of metal−alkene bonding in d^n metal complexes.

Scheme 1

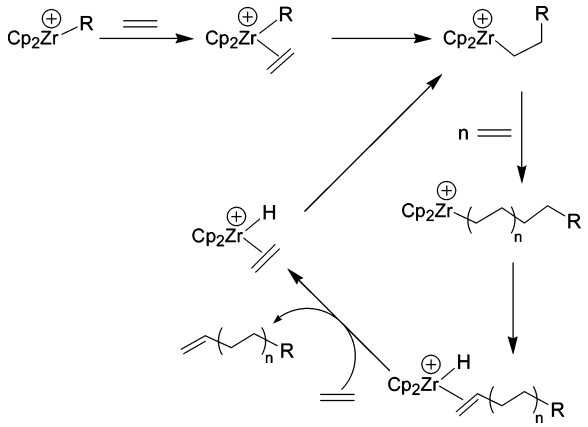

results in symmetrical alkene coordination, i.e., nearly identical $M-C_{vinyl}$ distances, even for unsymmetrical alkenes.[6] For d^0 metals, d−π* back-bonding is not possible,[7] and therefore

(1) (a) Mülhaupt, R. *Macromol. Chem. Phys.* **2003**, *204*, 289. (b) Resconi, L.; Cavallo, L.; Fait, A.; Piemontesi, F. *Chem. Rev.* **2000**, *100*, 1253. (c) Brintzinger, H. H.; Fischer, D.; Mülhaupt, R.; Rieger, B.; Waymouth, R. M. *Angew. Chem., Int. Ed. Engl.* **1995**, *34*, 1143.
(2) (a) Cossee, P. *Tetrahedron Lett.* **1960**, *17*, 12. (b) Cossee, P. *J. Catal.* **1964**, *3*, 80. (c) Arlman, E. J.; Cossee, P. *J. Catal.* **1964**, *3*, 99. (d) Brookhart, M.; Green, M. L. H. *J. Organomet. Chem.* **1983**, *250*, 395. (e) Grubbs, R. H.; Coates, G. W. *Acc. Chem. Res.* **1996**, *29*, 85.
(3) (a) Margl, P.; Deng, L.; Ziegler, T. *Top. Catal.* **1999**, *7*, 187. (b) Fan, L.; Harrison, D.; Woo, T. K.; Ziegler, T. *Organometallics* **1995**, *14*, 2018. (c) Lanza, G.; Fragalà, I. L. *Top. Catal.* **1999**, *7*, 45.
(4) (a) Woo, T. K.; Fan, L.; Ziegler, T. *Organometallics* **1994**, *13*, 2252. (b) Lauher, J. W.; Hoffmann, R. *J. Am. Chem. Soc.* **1976**, *98*, 1729.
(5) (a) Dewar, M. J. S. *Bull. Soc. Chim. Fr.* **1951**, *18*, C79. (b) Chatt, J.; Duncanson, L. A. *J. Chem. Soc.* **1953**, 2939. (c) Hartley, F. R. *Angew. Chem., Int. Ed. Engl.* **1972**, *11*, 596.
(6) Leading references: (a) Koelle, U.; Kang, B.-S.; Spaniol, T. P.; Englert, U. *Organometallics* **1992**, *11*, 249. (b) de Klerk-Engels, B.; Delis, J. G. P.; Vrieze, K.; Goubitz, K.; Fraanje, J. *Organometallics* **1994**, *13*, 3269. (c) Pedone, C.; Benedetti, E. *J. Organomet. Chem.* **1971**, *29*, 443. (d) Proft, B.; Pörschke, K.-R.; Lutz, F.; Krüger, C. *Chem. Ber.* **1991**, *124*, 2667. (e) Chirik, P. J.; Zubris, D. L.; Ackerman, L. J.; Henling, L. M.; Day, M. W.; Bercaw, J. E. *Organometallics* **2003**, *22*, 172.

10.1021/ja0575225 CCC: $33.50

Chart 1

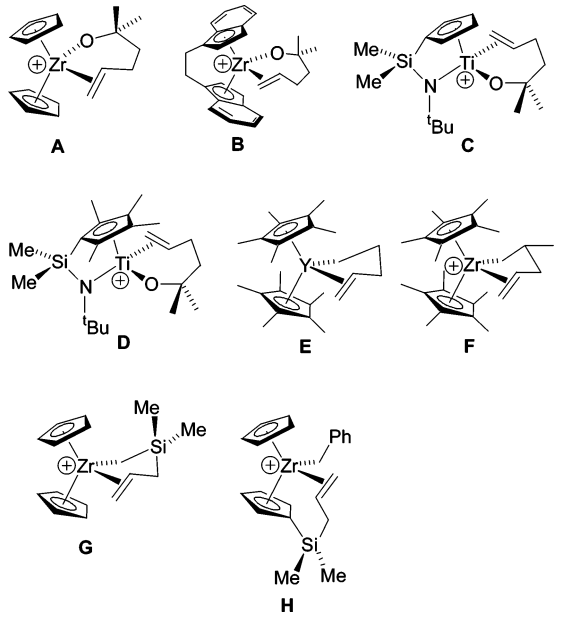

metal−alkene binding will be weak, and the complexes will be susceptible to ligand substitution reactions. The rapid insertion reactions and low metal−alkene bond strengths of d^0 metal−alkene complexes make these species challenging targets for study.

Jordan and co-workers reported detailed studies of chelated zirconium and titanium−alkene complexes $L_nM(OCMe_2CH_2CH_2CH{=}CH_2)^+$ (L_nM = Cp_2Zr (**A**); L_nM = *rac*-(EBI)Zr (**B**); EBI = 1,2-(1-indenyl)$_2$ethane; L_nM = ($C_5H_4SiMe_2N^tBu$)Ti (**C**); L_nM = ($C_5Me_4SiMe_2N^tBu$)Ti (**D**)) which are shown in Chart 1.[8] An X-ray crystallographic analysis of **B** showed that the alkene is coordinated in a highly unsymmetrical fashion that is essentially an η^1-alkene binding mode. For this species, d(Zr−C_{term}) = 2.634(5) Å, d(Zr−C_{int}) = 2.819(4) Å, and $\Delta d = d$(Zr−C_{int}) − d(Zr−C_{term}) = 0.185(6) Å. The structure of **A** is similar. Key NMR parameters for **A**−**D** include large downfield coordination shifts for H_{int} ($\Delta\delta = \delta_{coord} - \delta_{free}$ = 0.7−1.6) and C_{int} ($\Delta\delta$ = 18−25), and a large upfield coordination shift for C_{term} ($\Delta\delta$ = −11 − −22) with respect to the corresponding $L_nM(OCMe_2CH_2CH_2CH{=}CH_2)(THF)^+$ complexes in which the alkene is not coordinated. These results imply that the alkene is polarized with positive charge buildup on C_{int} and negative charge buildup on C_{term} as a result of the unsymmetrical binding. The $^1J_{CH}$ coupling constants of the vinyl unit are essentially unchanged by coordination, which indicates that the alkene structure is not significantly perturbed by coordination.

Casey studied chelated neutral d^0 yttrium−alkyl−alkene complexes (**E**)[9] and cationic zirconium−alkyl−alkene complexes (**F**),[10] in which the chelate ring size prevents alkene insertion. Casey and Bercaw described chelated d^0 zirconium−alkyl−alkene complexes that incorporate $SiMe_2$ units in the chelate arm to enhance coordination and prevent β-elimination reactions (**G**), and have studied the effects of alkene and Cp ligand substitution on the dynamics of these compounds.[11] Royo reported d^0 zirconium and hafnium−alkyl−alkene complexes in which a β-Si-substituted alkene is tethered to a Cp or indenyl ligand (**H**).[12] The NMR properties of **E**-**H** are similar to those of the structurally characterized examples **A** and **B**,[8] which suggests that unsymmetrical alkene coordination and concomitant polarization of the C=C bond may be a general feature of d^0 metal−alkene complexes.[13]

Chart 2

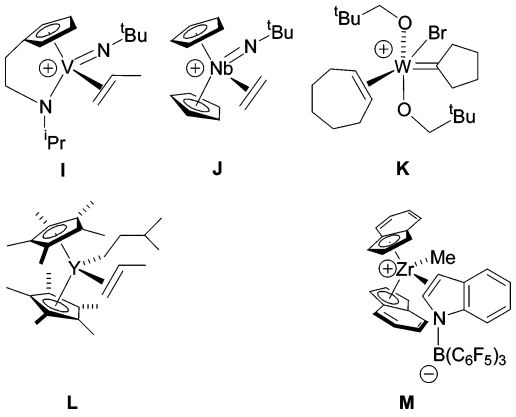

As chelation may influence the structure, dynamics, and reactivity of d^0 metal−alkene complexes, it is desirable to study *nonchelated* systems to probe the fundamental features of the d^0 metal−alkene interaction. Hessen[14] and Green[15] reported cationic vanadium− and niobium−imido−alkene complexes (**I** and **J**, Chart 2). The NMR coordination shifts of the propylene adducts of V^V and Nb^V are similar to those of **A** and **B**, again suggesting similar unsymmetrical alkene coordination. Kress observed several related tungsten−*alkylidene*−cycloalkene complexes (**K**) at low temperature.[16]

Nonchelated d^0 metal−alkyl−alkene species are very rare. Casey studied the coordination of propylene, 1-butene, and

(7) (a) Back-bonding from a metal−ligand bonding orbital is possible. For this effect in d^0 metal−carbonyl complexes, see: (b) Guo, Z.; Swenson, D. C.; Guram, A. S.; Jordan, R. F. *Organometallics* **1994**, *13*, 766. (c) Marsella, J. A.; Curtis, C. J.; Bercaw, J. E.; Caulton, K. G. *J. Am. Chem. Soc.* **1980**, *102*, 7244.

(8) (a) Wu, Z.; Jordan, R. F.; Petersen, J. L. *J. Am. Chem. Soc.* **1995**, *117*, 5867. (b) Carpentier, J. F.; Wu, Z.; Lee, C. W.; Strömberg, S.; Christopher, J. N.; Jordan, R. F. *J. Am. Chem. Soc.* **2000**, *122*, 7750. (c) Carpentier, J.-F.; Maryin, V. P.; Luci, J.; Jordan, R. F. *J. Am. Chem. Soc.* **2001**, *123*, 898.

(9) (a) Casey, C. P.; Carpenetti, D. W., II; Sakurai, H. *J. Am. Chem. Soc.* **1999**, *121*, 9483. (b) Casey, C. P.; Carpenetti, D. W., II. *Organometallics* **2000**, *19*, 3970.

(10) (a) Casey, C. P.; Klein, J. F.; Fagan, M. A. *J. Am. Chem. Soc.* **2000**, *122*, 4320. (b) Casey, C. P. Fagan, M. A.; Hallenbeck, S. L. *Organometallics* **1998**, *17*, 287. (c) Casey, C. P.; Fisher, J. J. *Inorg. Chim. Acta* **1998**, *270*, 5. (d) Casey, C. P.; Hallenbeck, S. L.; Wright, J. M.; Landis, C. R. *J. Am. Chem. Soc.* **1997**, *119*, 9680. (e) Casey, C. P.; Hallenbeck, S. L.; Pollock, D. W.; Landis, C R. *J. Am. Chem. Soc.* **1995**, *117*, 9770.

(11) (a) Brandow, C. G.; Mendiratta, A.; Bercaw, J. E. *Organometallics* **2001**, *20*, 4253. (b) Casey, C. P.; Carpenetti, D. W., II; Sakurai, H. *Organometallics* **2001**, *20*, 4262.

(12) (a) Martínez, G.; Royo, P. *Organometallics* **2005**, *24*, 4782. (b) Cano, J.; Gómez-Sal, P.; Heinz, G.; Martínez, G.; Royo, P. *Inorg. Chim. Acta* **2003**, *345*, 15. (c) Galakhov, M. V.; Heinz, G.; Royo, P. *Chem. Commun.* **1998**, 17.

(13) Other chelated d^0 metal−alkene complexes: (a) Horton, A. D.; Orpen, A. G. *Organometallics* **1992**, *11*, 8. (b) Erker, G. *Acc. Chem. Res.* **2001**, *34*, 309. (c) Dahlmann, M.; Erker, G.; Bergander, K. *J. Am. Chem. Soc.* **2000**, *122*, 7986. (d) Karl, J.; Dahlmann, M.; Erker, G.; Bergander, K. *J. Am. Chem. Soc.* **1998**, *120*, 5643. (e) Karl, J.; Erker, G. *J. Mol. Catal. A: Chem.* **1998**, *128*, 85. (f) Basuli, F.; Bailey, B. C.; Watson, L. A.; Tomaszewski, J.; Huffman, J. C.; Mindiola, D. J. *Organometallics* **2005**, *24*, 1886. (g) Ruwwe, J.; Erker, G.; Fröhlich, R. *Angew. Chem., Int. Ed. Engl.* **1996**, *35*, 80. (h) Yoshida, M.; Jordan, R. F. *Organometallics* **1997**, *16*, 4508. (i) Evans, W. J.; Kozimor, S. A.; Brady, J. C.; Davis, J. C.; Nyce, G. W.; Seibel, C. A.; Ziller, C. A.; Doedens, R. J. *Organometallics* **2005**, *24*, 2269. (j) Yamada, J.; Nomura, K. *Organometallics* **2005**, *24*, 3621.

(14) Witte, P. T.; Meetsma, A.; Hessen, B.; Budzelaar, P. H. M. *J. Am. Chem. Soc.* **1997**, *119*, 10561.

(15) Humphries, M. J.; Douthwaite, R. E.; Green, M. L. H. *J. Chem. Soc., Dalton Trans.* **2000**, 2952.

(16) Kress, J.; Osborn, J. A. *Angew. Chem., Int. Ed. Engl.* **1992**, *31*, 1585.

1-hexene to Cp^*_2YR ($Cp^* = C_5Me_5$).[17] Low-temperature NMR spectra of mixtures of Cp^*_2YR and alkenes contain one set of exchange-averaged alkene signals that shift in same directions as observed for chelated yttrium−alkene compounds.[10] These results imply that Cp^*_2YR(alkene) adducts (**L**) are formed and undergo fast intermolecular exchange with free alkene on the NMR time scale. Resconi characterized an [(indenyl)$_2$ZrMe]-[indole·B(C_6F_5)$_3$] ion pair (**M**), which NMR evidence implies is held together by η^2-C=C indole coordination.[18]

In addition to these d^0 transition metal−alkene complexes, other alkene complexes in which π-back-bonding is absent have been reported, including chelated metal−alkene adducts of alkali metals,[19] alkaline earth metals,[20] Sm^{III},[21] and Al, Ga, and In,[22] as well as norbornyl-type cations in which an alkene is coordinated to Si, Ge, Sn, or Pb.[23] The ion pair [Bu_3Sn][H_2C=$CHCH_2B(C_6F_5)_3$], which is generated from B(C_6F_5)$_3$ and Bu_3SnCH_2CH=CH_2, may be viewed as an alkene complex of Bu_3Sn^+ and exhibits NMR properties that are similar to those of d^0 transition metal−alkene complexes.[24] Metal−alkene complexes in which back-bonding is very weak, such as Ag^I systems,[25] are also known.[26]

This paper describes the generation and properties of non-chelated $Cp'_2Zr(O^tBu)(alkene)^+$ ($Cp' = C_5H_4Me$) and $Cp_2Zr(O^tBu)(alkene)^+$ complexes. These species are models for the $(C_5R_5)_2Zr(polymeryl)(alkene)^+$ intermediates in Zr-catalyzed alkene polymerization reactions.[27]

Results

Targets. The objective of this work was to study nonchelated alkene complexes of the d^0-metal species $(C_5H_4R)_2Zr(O^tBu)^+$ (R = H, Me), to probe the Zr^{IV}−alkene interaction. The *tert*-butoxide ligand was used to provide stable, electrophilic zirconocene species that cannot undergo alkene insertion, due to the strong Zr−O bond,[28] and to enable direct comparisons with the chelated systems **A** and **B**.[8] The Cp′ ligand provides a convenient symmetry probe to facilitate identification of reactive species and characterization of exchange processes. The $B(C_6F_5)_4^-$ anion was chosen for its weak coordinating ability[29] and low reactivity with zirconocene cations.[30]

Scheme 2. Anion = $B(C_6F_5)_4^-$

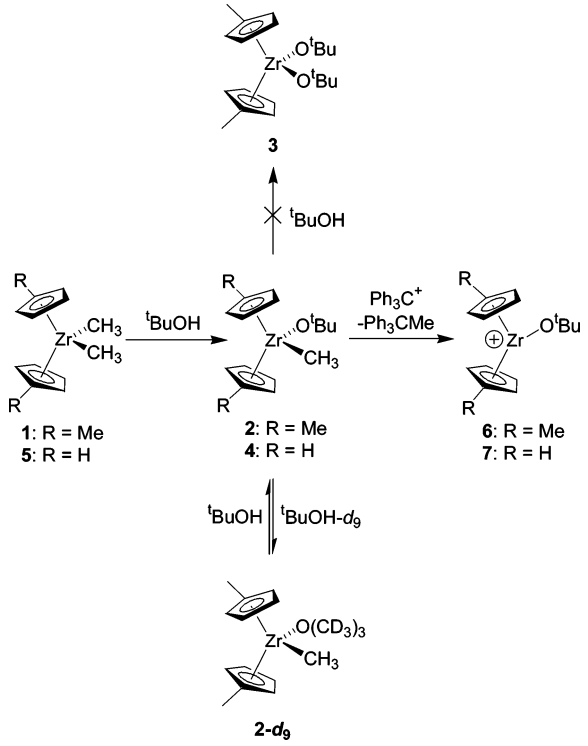

$(C_5H_4R)_2Zr(O^tBu)Me$ Complexes. The reaction of Cp'_2ZrMe_2 (**1**) with excess ^{t}BuOH in benzene produces $Cp'_2Zr(O^tBu)Me$ (**2**) within 15 min at 22 °C (Scheme 2).[31] No further reaction of **2** with ^{t}BuOH to give $Cp'_2Zr(O^tBu)_2$ (**3**) occurs after 3 d under these conditions. However, treatment of **2** with ^{t}BuOH-d_9 resulted in an equilibrium mixture of **2**, $Cp'_2Zr(OC(CD_3)_3)Me$ (**2-d_9**), ^{t}BuOH, and ^{t}BuOH-d_9 within 1 h ($K_1 = 0.99(4)$, C_6D_6, 22 °C).[32] This result shows that protonolysis of the Zr−O^tBu bond of **2** is favored over protonolysis of the Zr−CH_3 bond, probably due to the availability of the lone pairs on the alkoxide ligand. Similar kinetic basicity effects have been observed in reactions of zirconium alkoxides and zirconium alkyls with hydroxylated Al and Si surfaces, and in the reaction of $MeAl(O\text{-}2,6\text{-}^tBu\text{-}4\text{-}Me\text{-}Ph)_2$ with H_2O.[33] The analogous compound $Cp_2Zr(O^tBu)Me$ (**4**) was generated from Cp_2ZrMe_2 (**5**) on an NMR scale by the procedure used for **2**. Compounds **2** and **4** are C_s symmetric in solution, and exhibit $OCMe_3$ ^{13}C NMR signals at δ 76.9 and 77.1, respectively.

$(C_5H_4R)_2Zr(O^tBu)^+$ Species. Compounds **2** and **4** react with $[Ph_3C][B(C_6F_5)_4]$[30b] in C_6D_5Cl or C_6H_6 within 15 min at 22 °C to yield cationic Zr−alkoxide species $[(C_5H_4R)_2Zr(O^tBu)][B(C_6F_5)_4]$ (**6**: R = Me; **7**: R = H), as shown in Scheme 2.[34]

(17) (a) Casey, C. P.; Tunge, J. A.; Lee, T.-Y.; Fagan, M. A. *J. Am. Chem. Soc.* **2003**, *125*, 2641. (b) Casey, C. P.; Lee, T.-Y.; Tunge, J. A.; Carpenetti, D. W., II. *J. Am. Chem. Soc.* **2001**, *123*, 10762.
(18) Bonazza, A.; Cumurati, I.; Guidotti, S.; Mascellari, N.; Resconi, L. *Macromol. Chem. Phys.* **2004**, *205*, 319.
(19) (a) Evans, W. J.; Brady, J. C.; Fujimoto, C. H.; Giarikos, D. G.; Ziller, J. W. *J. Organomet. Chem.* **2002**, *649*, 252. (b) Hu, J.; Barbour, L. J.; Gokel, G. W. *Chem. Commun.* **2001**, 1858.
(20) Schumann, H.; Schutte, S.; Kroth, H.-J.; Lentz, D. *Angew. Chem., Int. Ed.* **2004**, *43*, 6208.
(21) Evans, W. J.; Perotti, J. W.; Brady, J. C.; Ziller, J. W. *J. Am. Chem. Soc.* **2003**, *125*, 5204.
(22) (a) Hata, G. *Chem. Commun.* **1968**, 7. (b) Dolzine, T. W.; Oliver, J. P. *J. Am. Chem. Soc.* **1974**, *96*, 1737. (c) Pietryga, J. M.; Jones, J. N.; Mullins, L. A.; Wiacek, R. J.; Cowley, A. H. *Chem. Commun.* **2003**, 2072.
(23) (a) Steinberger, H.-U.; Müller, T.; Auner, N.; Maerker, C.; von Ragué Schleyer, P. *Angew. Chem., Int. Ed. Engl.* **1997**, *36*, 626. (b) Müller, T.; Bauch, C.; Bolte, M.; Auner, N. *Chem. Eur. J.* **2003**, *9*, 1746. (c) Müller, T.; Bauch, C.; Ostermeier, M.; Bolte, M.; Auner, N. *J. Am. Chem. Soc.* **2003**, *125*, 2158.
(24) (a) Blackwell, J. M.; Piers, W. E.; McDonald, R. *J. Am. Chem. Soc.* **2002**, *124*, 1295. (b) Blackwell, J. M.; Piers, W. E.; Parvez, M. *Org. Lett.* **2000**, *2*, 695.
(25) Hurlburt, P. K.; Rack, J. J.; Luck, J. S.; Dec, S. F.; Webb, J. D.; Anderson, O. P.; Strauss, S. H. *J. Am. Chem. Soc.* **1994**, *116*, 10003.
(26) (a) Krossing, I.; Reisinger, A. *Angew. Chem., Int. Ed.* **2003**, *42*, 5725. (b) Dias, H. V. R.; Wang, Z.; Jin, W. *Inorg. Chem.* **1997**, *36*, 6205. (c) Dias, H. V. R.; Wang, X. *J. Chem. Soc., Dalton Trans.* **2005**, 2985. (d) Aris, K. R.; Aris, V.; Brown, J. M. *J. Organomet. Chem.* **1972**, *42*, C67. (e) Evans, W. J.; Giarikos, D. G.; Josell, D.; Ziller, J. W. *Inorg. Chem.* **2003**, *42*, 8255.
(27) For preliminary communications, see: (a) Stoebenau, E. J., III; Jordan, R. F. *J. Am. Chem. Soc.* **2003**, *125*, 3222. (b) Stoebenau, E. J., III; Jordan, R. F. *J. Am. Chem. Soc.* **2004**, *126*, 11170.
(28) (a) Lappert, M. F.; Patil, D. S.; Pedley, J. B. *Chem. Commun.* **1975**, 830. (b) Schock, L. E.; Marks, T. J. *J. Am. Chem. Soc.* **1988**, *110*, 7701.
(29) (a) Krossing, I.; Raabe, I. *Angew. Chem., Int. Ed.* **2004**, *43*, 2066. (b) Strauss, S. H. *Chem. Rev.* **1993**, *93*, 927. (c) Chen, E. Y.-X.; Marks, T. J. *Chem. Rev.* **2000**, *100*, 1391. (d) Turner, H. W. Eur. Patent EP0277004, 1988. (e) Massey, A. G.; Park, A. J. *J. Organomet. Chem.* **1964**, *1*, 245.
(30) (a) Krossing, I.; Raabe, I. *Chem. Eur. J.* **2004**, *10*, 5017. (b) Chien, J. C. W.; Tsai, W.-M.; Rausch, M. D. *J. Am. Chem. Soc.* **1991**, *113*, 8570.
(31) Brandow, C. G. Zirconocenes as Models for Homogeneous Ziegler−Natta Olefin Polymerization Catalysts. Ph.D. Thesis, California Institute of Technology, Pasadena, CA, 2001.
(32) $K_1 = [\mathbf{2}\text{-}d_9][^t\text{BuOH}][\mathbf{2}]^{-1}[^t\text{BuOH}\text{-}d_9]^{-1}$.
(33) (a) Miller, J. B.; Schwartz, J.; Bernasek, S. L. *J. Am. Chem. Soc.* **1993**, *115*, 8239. (b) Stapleton, R. A.; Galan, B. R.; Collins, S.; Simons, R. S.; Garrison, J. C.; Youngs, W. J. *J. Am. Chem. Soc.* **2003**, *125*, 9246.

Scheme 3

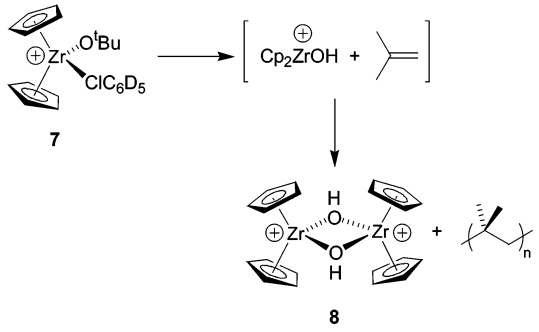

7 **8**

Compound **6** was isolated as a pale-yellow, base-free solid by washing with benzene to remove Ph_3CMe, followed by washing with hexanes and vacuum drying. Complex **7** was generated and used in situ. The ^{13}C NMR $OCMe_3$ resonances in C_6D_5Cl of **6** (δ 84.1) and **7** (δ 84.6) are shifted ca. 7 ppm downfield from the corresponding signals of **2** and **4**.

Compound **6** is a weaker Lewis acid than the related alkyl cation Cp'_2ZrMe^+. Competition experiments show that THF preferentially binds to Cp'_2ZrMe^+ over **6**.[35] In addition, the dinuclear intermediate $\{Cp'_2Zr(O^tBu)\}_2(\mu\text{-Me})^+$ is not observed when reactions of **2** and Ph_3C^+ are monitored by NMR spectroscopy,[36] while $\{Cp'_2ZrMe\}_2(\mu\text{-Me})^+$ is observed in the reactions of **1** with Ph_3C^+.[37]

Compound **6** is very stable in C_6D_5Cl solution at 22 °C (no decomposition after 7 d) and in the solid state at −35 °C (no decomposition after 1 year). Compound **6** is also stable for at least 8 h at −89 °C in CD_2Cl_2, but decomposes completely within 17 h at 22 °C in this solvent to unknown products. Compound **7** is less stable than **6** and decomposes completely within 5 d at 22 °C in C_6D_5Cl solution to poly(isobutene) and the dinuclear dicationic complex $[\{Cp_2Zr\}_2(\mu\text{-OH})_2][B(C_6F_5)_4]_2$ (**8**), which separates as yellow crystals. Compound **8** forms by net isobutene elimination from **7**, as shown in Scheme 3. The isobutene is cationically polymerized under the reaction conditions, and $Cp_2Zr(OH)^+$ dimerizes to **8**. A similar decomposition reaction was observed for $Cp_2Zr(S^tBu)(THF)^+$.[38]

Molecular Structure of $\{Cp_2Zr\}_2(\mu\text{-OH})_2^{2+}$. The structure of **8** was determined by X-ray crystallography. The dication consists of two normal bent zirconocene units linked by two bridging hydroxide groups (Figure 2).[39] The Zr_2O_2 core is planar. The Zr−O bond lengths (2.161(3) and 2.158(2) Å) are similar those in other complexes with $Zr_2(\mu\text{-OH})_2$ cores, such as $\{Cp_2Zr(OCOCF_3)(\mu\text{-OH})\}_2$ (**9**), $(Cp_2Zr\{imidazole{\cdot}B(C_6F_5)_3\})_2(\mu\text{-OH})_2$ (**10**), and $[\{Cp_2Zr(NC^nPr)\}_2(\mu\text{-OH})_2][BPh_4]_2$ (**11**).[40] The O−Zr−O angle in **8** (72.0(1)°) is 6−7° larger, and the Zr−O−Zr angle (108.0(1)°) is 6−7° smaller than the corresponding angles in **9**−**11**, where an additional ligand is present.[40a−c] There is a close contact (2.24 Å) between the hydroxide proton and a *m*-fluorine of the anion in **8**, which is less than the sum of the hydrogen and fluorine van der Waals radii (2.67 Å).[41]

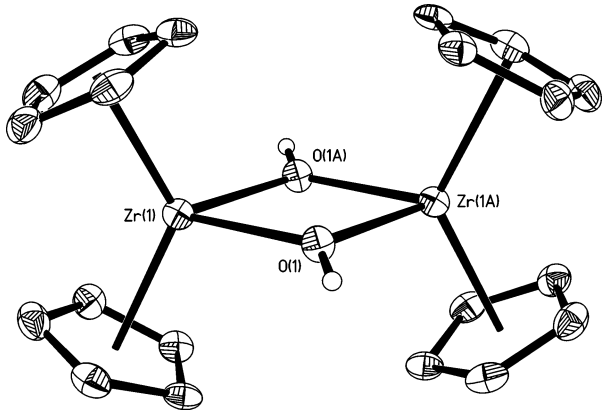

Figure 2. ORTEP view (50% probability ellipsoids) of the structure of the $(Cp_2Zr)_2(\mu\text{-OH})_2^{2+}$ dication of **8**. Hydrogen atoms on the Cp rings are omitted.

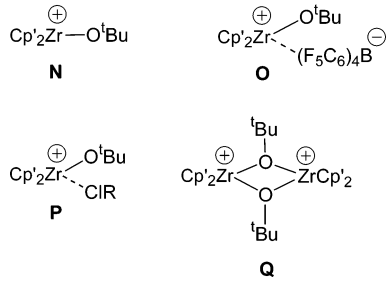

Figure 3. Possible solution structures for **6**.

Solution Structure of $(C_5H_4R)_2Zr(O^tBu)^+$ Cations. The ^1H and ^{13}C NMR spectra of **6** in CD_2Cl_2 each contain two Cp′ CH signals, even at −89 °C, indicative of C_{2v} symmetry. This result suggests four possible solution structures for **6**. First, **6** may contain a three-coordinate $Cp'_2Zr(O^tBu)^+$ cation in which the alkoxide ligand occupies the central coordination site in the zirconocene wedge (**N**, Figure 3), similar to $Cp^*_2Sm(O\text{-}2,3,5,6\text{-}Me_4\text{-}Ph)$,[42] or exchanges rapidly between the sides of the zirconocene wedge. Second, **6** may be a contact ion pair (**O**), which undergoes fast site epimerization at Zr (i.e. fast exchange of the *tert*-butoxide ligand and anion between the sides of the zirconocene wedge). Coordination of $B(C_6F_5)_4^-$ to electrophilic Zr, Th, Al, and Sc cations is known.[43] Third, **6** may be a solvent adduct (**P**), which undergoes rapid site epimerization at Zr. Several d^0 metal−haloarene complexes have been characterized, including $Cp_2Zr(CH_2Ph)(ClPh)^+$, $Cp^*_2ZrCl(ClPh)^+$, Cp^*_2Sc-

(34) For related $(C_5R_5)_2Zr(OR)(L)^+$ species, see: (a) Collins, S.; Koene, B. E.; Ramachandran, R.; Taylor, N. J. *Organometallics* **1991**, *10*, 2092. (b) Hong, Y.; Kuntz, B. A.; Collins, S. *Organometallics* **1993**, *12*, 964. (c) Hong, Y.; Norris, D. J.; Collins, S. *J. Org. Chem.* **1993**, *58*, 3591. (d) Jordan, R. F.; Dasher, W. D.; Echols, S. F. *J. Am. Chem. Soc.* **1986**, *108*, 1718.

(35) For the **6** + $Cp'_2ZrMe(THF)^+ \leftrightarrows Cp'_2Zr(O^tBu)(THF)^+ + Cp'_2ZrMe^+$ equilibrium, $K_2 = [ZrOR(THF)][ZrMe][\mathbf{6}]^{-1}[ZrMe(THF)]^{-1} = 0.34(6)$ in C_6D_5Cl at 22 °C.

(36) $\{Cp'_2Zr(O^tBu)\}_2(\mu\text{-Me})^+$ can be generated from a 2:1 mixture of **2** and $[Ph_3C][B(C_6F_5)_4]$ in C_6D_5Cl.

(37) (a) Bochmann, M.; Lancaster, S. J. *Angew. Chem., Int. Ed. Engl.* **1994**, *33*, 1634. (b) Wu, F.; Dash, A. K.; Jordan, R. F. *J. Am. Chem. Soc.* **2004**, *126*, 15360.

(38) Piers, W. E.; Koch, L.; Ridge, D. S.; MacGillivray, L. R.; Zaworotko, M. *Organometallics* **1992**, *11*, 3148.

(39) Cardin, D. J.; Lappert, M. F.; Raston, C. L. *Chemistry of Organo-Zirconium and −Hafnium Compounds*; Ellis Horwood Ltd: Chichester, U.K., 1986; pp 68−75.

(40) (a) Klima, S.; Thewalt, U. *J. Organomet. Chem.* **1988**, *354*, 77. (b) Röttger, D.; Erker, G.; Fröhlich, R.; Kotila, S. *J. Organomet. Chem.* **1996**, *518*, 17. (c) Aslan, H.; Eggers, S. H.; Fischer, R. D. *Inorg. Chim. Acta* **1989**, *159*, 55. (d) Martin, A.; Uhrhammer, R.; Gardner, T. G.; Jordan, R. F.; Rogers, R. D. *Organometallics* **1998**, *17*, 382.

(41) Porterfield, W. W. *Inorganic Chemistry: A Unified Approach*, 2nd ed.; Academic Press: San Diego, 1993; p 214.

(42) Evans, W. J.; Hanusa, T. P.; Levan, K. R. *Inorg. Chim. Acta* **1985**, *110*, 191.

(43) (a) Goodman, J. T.; Schrock, R. R. *Organometallics* **2001**, *20*, 5205. (b) Yang, X.; Stern, C. L.; Marks, T. J. *Organometallics* **1991**, *10*, 840. (c) Korolev, A. V.; Delpech, F.; Dagorne, S.; Guzei, I. A.; Jordan, R. F. *Organometallics* **2001**, *20*, 3367. (d) Bouwkamp, M. W.; Budzelaar, P. H. M.; Gercama, J.; Del Hierro Morales, I.; de Wolf, J.; Meetsma, A.; Troyanov, S. I.; Teuben, J. H.; Hessen, B. *J. Am. Chem. Soc.* **2005**, *127*, 14310.

$(FPh)_2^+$, and $Cp^*_2Sc(\kappa^2\text{-}o\text{-}F_2C_6H_4)^+$.[37b,43d,44] Finally, **6** may be a dinuclear dication with two bridging *tert*-butoxide ligands (**Q**) analogous to **8**. Dinuclear yttrium and chromium complexes with μ-O^{t}Bu ligands are known,[45] and smaller alkoxides can bridge between Zr centers.[40d]

The reaction of a 1:1 mixture of **2** and **4** with $[Ph_3C][B(C_6F_5)_4]$ (1 equiv based on total Zr) gives only **6** and **7**. No new resonances or line broadening effects are observed in NMR spectra of the product mixture that can be ascribed to a mixed $Cp_2Zr(\mu\text{-}O^tBu)_2ZrCp'_2{}^{2+}$ complex, which would be expected to form if **6** and **7** contained dinuclear dications. This result implies that **6** and **7** do not contain dinuclear dications of type **Q**.

Differentiation between structures **N**−**P** is more difficult. Addition of PhCl or C_6D_5Cl to CD_2Cl_2 solutions of **6** at −89 °C leads to selective shifts in the ^{1}H NMR Cp′-C*H* and O^{t}Bu resonances of **6**. Moreover, the coordination of ethylene to **6** in CD_2Cl_2 solution is perturbed by addition of PhCl but is not affected by addition of $[Ph_3C][B(C_6F_5)_4]$ as an anion source (vide infra). Finally, the ^{19}F NMR spectrum of **6** shows no evidence of anion coordination to Zr down to −89 °C, although the effects of weak, labile anion coordination on the ^{19}F NMR spectrum may be subtle. Collectively, these results are most consistent with **6** and **7** existing as halocarbon adducts of type **P** in halocarbon solution.

Generation of Cp′$_2$Zr(O^{t}Bu)(alkene)$^+$ Complexes. The addition of excess alkene to a CD_2Cl_2 solution of **6** at low temperature produces an equilibrium mixture of $[Cp'_2Zr(O^tBu)(alkene)][B(C_6F_5)_4]$ (**12a**−**l**), **6**, and free alkene, as shown in eq 1. In a typical experiment, the alkene was added by vacuum transfer to a frozen solution of **6** in CD_2Cl_2 in an NMR tube. The tube was thawed, stored at −78 °C, and transferred to a precooled NMR probe with minimal transfer time (<1 min) to minimize side reactions. Alkene complexes **12a**−**l** were characterized by NMR spectroscopy. These species are thermally sensitive, which precluded isolation or ESI-MS analysis.

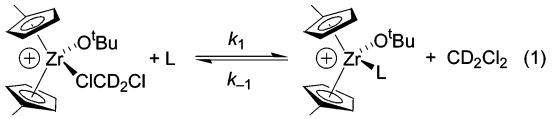

6 **12a-l**

anion = $B(C_6F_5)_4^{\ominus}$

cpd	L
a	$H_2C{=}CH_2$
b	$H_2C{=}CHMe$
c	$H_2C{=}CH^nBu$
d	$H_2C{=}CHCH_2CH_2CH{=}CH_2$
e	$H_2C{=}CHCH_2{}^tBu$
f	$H_2C{=}CHO^tBu$
g	$H_2C{=}CHCH_2SiMe_3$
h	$H_2C{=}CHC_5H_4FeCp$
i	$H_2C{=}C{=}CH_2$
j	*cis*-MeHC=CHMe
k	cyclopentene
l	$H_2C{=}CHCl$

Side reactions complicated studies of the binding of certain alkenes to **6**. Ethylene polymerization occurs above −40 °C in the presence of **6**, most likely due to the presence of trace Zr−alkyl species, though adduct **12a** could be studied up to this temperature. Addition of isobutene or styrene to **6** results in rapid cationic polymerization of the alkene at −78 °C, and the target Zr−isobutene or Zr−styrene adducts were not detected.[46] In the case of *tert*-butyl vinyl ether, cationic polymerization competes with π-complex formation, but the π-complex **12f** was observed. Finally, trace oxidation of vinylferrocene occurs during the formation of **12h**, probably due to the presence of trace Ph_3C^+ in **6**.[47]

NMR Properties and Solution Structures of Cp′$_2$Zr(O^{t}Bu)(alkene)$^+$ Complexes. (A) General Features. The ^{1}H and ^{13}C{^{1}H} NMR spectra of **12a**,**j**,**k**, which contain symmetrical alkenes, each contain four Cp′ CH resonances, one Cp′ ipso-C resonance, and one Cp′*Me* resonance, consistent with C_s-symmetric structures. The ^{1}H and ^{13}C spectra of **12a** contain a single coordinated-ethylene resonance, even at −89 °C. This result implies that the bound ethylene rotates around the Zr−(ethylene centroid) axis rapidly on the NMR time scale. The NMR spectra of **12j**,**k** contain one set of =CHR resonances (i.e. the ends of the alkene are equivalent) which, along with the C_s symmetry, is consistent with fast rotation around the Zr−(alkene centroid) axis or a static structure in which the alkene C=C bond is perpendicular to the O−Zr−(alkene centroid) plane, which is unlikely on steric grounds.[48]

The NMR spectra of **12b**−**h**, which contain monosubstituted alkenes, each contain eight Cp′ CH resonances, two Cp′ ipso-C resonances, and two Cp′*Me*[49] resonances at −89 °C, characteristic of C_1 symmetry. The Cp′ rings are diastereotopic due to the chiral center at C_{int} of the bound alkene. The NMR spectra of **12b**−**h** contain a single set of alkene resonances, which is consistent with the presence of a single rotamer or, more likely, fast metal−(alkene centroid) rotation.[48]

(B) Monosubstituted Alkene Adducts. The alkene ^{13}C NMR resonances of monosubstituted alkene complexes **12b**−**h** display characteristic coordination shifts that are listed in Table 1. The C_{int} resonances shift downfield by 15−30 ppm, while the C_{term} resonances shift upfield by 10−25 ppm, compared to the free alkene positions. The vinyl region of the ^{13}C{^{1}H} NMR spectrum of propylene adduct **12b** is shown in Figure 4 and illustrates the divergent coordination shifts of the two vinyl resonances.

The ^{1}H NMR resonances for the vinyl units of **12b**−**h** are also strongly perturbed by coordination, as summarized in Table 1. The H_{int} signals shift far downfield ($\Delta\delta$ = 1.5−1.8) upon coordination, while the H_{trans} and H_{cis} resonances display smaller coordination shifts. The $^1J_{CH}$ coupling constants of the vinyl units of **12b**−**h** are only slightly perturbed by coordination (Table 2), and the vinyl $^nJ_{HH}$ coupling constants are essentially unchanged the from free alkene values.

The NMR properties of **12b**−**h** are very similar to those of structurally characterized chelated Zr^{IV}−alkoxide−alkene complexes **A** and **B**,[8] and thus imply that the alkene is bound in a similar unsymmetrical fashion (i.e. $d(Zr{-}C_{int}) > d(Zr{-}C_{term})$) and is polarized with positive charge buildup on C_{int} and negative charge buildup on C_{term}, as shown in Figure 5. The

(44) Bochmann, M.; Jaggar, A. J.; Nicholls, J. C. *Angew. Chem., Int. Ed. Engl.* **1990**, *29*, 780.
(45) (a) Evans, W. J.; Boyle, T. J.; Ziller, J. W. *Organometallics* **1993**, *12*, 3998. (b) Chisholm, M. H.; Cotton, F. A.; Extine, M. W.; Rideout, D. C. *Inorg. Chem.* **1979**, *18*, 120.
(46) η^2-Isobutene and η^2-styrene adducts of V^V are known. Witte, P. T. Vanadium Complexes Containing Amido Functionalized Cyclopentadienyl Ligands. Ph.D. Thesis, University of Groningen, Groningen, The Netherlands, 2000.
(47) Trace oxidation of ferrocene also occurs in the presence of **6** under similar conditions (CD_2Cl_2, −91 °C). It is probable that trace Ph_3C^+ is the oxidant.
(48) To date, NOESY spectra have not enabled clarification of this issue.
(49) The ^{1}H NMR Cp′*Me* resonances of **12b**−**h** often overlap.

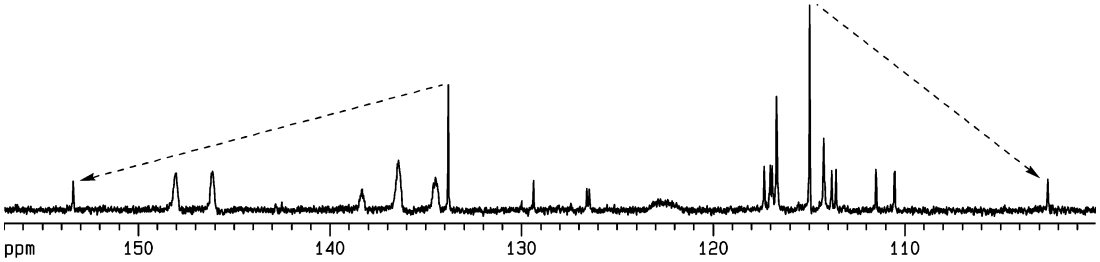

Figure 4. Partial $^{13}C\{^1H\}$ NMR spectrum of an equilibrium mixture of **12b**, **6**, and free propylene (CD_2Cl_2, −89 °C). Propylene coordination shifts are shown by arrows. Assignments: δ 154 (**12b** C_{int}), 147 (d, anion), 137 (d, anion), 136 (d, anion), 134 (C_3H_6 C_{int}), 129 (**6** C_{ipso}), 127 (2 s, **12b** C_{ipso}), 123 (br, anion), 117 (4 s, **12b** Cp′ CH), 117 (large s, **6** Cp′ CH), 115 (C_3H_6 C_{term}), 114 (**6** Cp′ CH), 114−111 (4 s, **12b** Cp′ CH), 103 (**12b** C_{term}).

Table 1. NMR Coordination Shifts ($\Delta\delta$) for Monosubstituted Alkenes Coordinated to **6**[a]

cpd	alkene	C_{int}	C_{term}	$C_{allylic}$	H_{int}	H_{trans}	H_{cis}
12b	propylene	19.6	−12.4	3.0	1.55	0.37	0.14
12c	1-hexene	17.5	−11.9	2.4	1.53	0.41	0.12
12d	1,5-hexadiene[b]	16.7	−11.3	2.2	1.46	0.38	x[c]
12e	4,4-Me_2-1-pentene	18.8	−11.7	1.5	1.46	0.38	0.24
12f	*t*-butyl vinyl ether	32.5	−23.8	—	1.58	−0.26	−0.21
12g	allyltrimethylsilane	31.6	−19.7	9.0	1.80	0.00	0.00
12h	vinylferrocene	30.3	−27.8	—	1.77	−0.56	−0.52

[a] In CD_2Cl_2, −89 °C; $\Delta\delta = \delta_{coord} - \delta_{free}$. [b] Values for the bound vinyl unit are shown; values for the pendant vinyl unit are essentially unchanged from free substrate values. [c] Resonance not detected due to overlap with free alkene resonance.

Table 2. $^1J_{CH}$ Coupling Constants (Hz) for Monosubstituted Alkenes Coordinated to **6**[a]

cpd	alkene	C_{int} coord	free	C_{term} coord	free
12b	propylene	156	153	156	155
12c	1-hexene	156	151	156	155
12d	1,5-hexadiene[b]	155	150	157	155
12e	4,4-Me_2-1-pentene	150	150	150	156, 154
12f	*tert*-butyl vinyl ether	173	174	154	161, 155
12g	allyltrimethylsilane	150	150	153	157, 153
12h	vinylferrocene	156	155	153	159, 155

[a] Values from $^{13}C\{gated-^1H\}$ NMR spectra; in CD_2Cl_2, −89 °C. [b] Values for the bound vinyl unit are shown; values for the pendant vinyl unit are essentially unchanged from free substrate values.

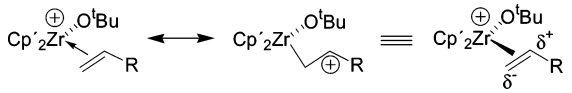

Figure 5. Polarization of the C═C bond of the alkene in $Cp'_2Zr(O^tBu)$-(alkene)$^+$ complexes.

C═C polarization explains the downfield coordination shifts of the C_{int}, H_{int}, and $C_{allylic}$ resonances and the upfield coordination shifts of the C_{term} resonances. The $^1J_{CH}$ values imply that the vinyl units of **12b**−**h** are not significantly structurally distorted (i.e. the hybridization at C_{int} and C_{term} is not significantly perturbed) by coordination.[50]

As summarized in Table 1, the coordination shifts for the C_{int}, C_{term}, and H_{int} of the *tert*-butyl vinyl ether (**12f**), vinylferrocene (**12h**), and allyltrimethylsilane (**12g**) adducts are larger than those for simple alkene complexes **12b**−**e**. Additionally, the H_{trans} and H_{cis} resonances of **12f**−**h** are shifted less downfield than those in **12b**−**e**, and in some cases exhibit upfield

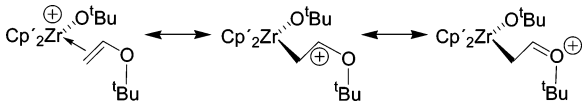

Figure 6. Resonance stabilization of $Cp'_2Zr(O^tBu)(\eta^2\text{-}H_2C{=}CHO^tBu)^+$ (**12f**).

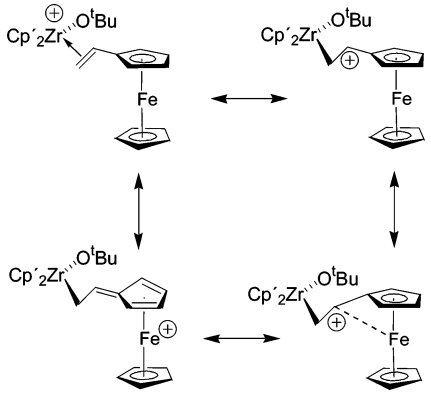

Figure 7. Resonance stabilization of $Cp'_2Zr(O^tBu)(H_2C{=}CHC_5H_4FeCp)^+$ (**12h**).

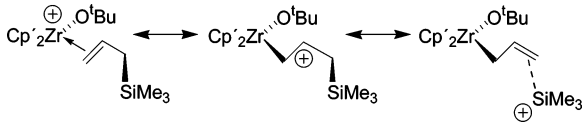

Figure 8. β-Si stabilization of $Cp'_2Zr(O^tBu)(H_2C{=}CHCH_2SiMe_3)^+$ (**12g**).

coordination shifts. Enhanced polarization of the alkene C═C bond in **12f**−**h** due to resonance effects (Figures 6 and 7)[51] or β-Si hyperconjugation (Figure 8),[52] which stabilizes the partial positive charge on C_{int}, explains these coordination shifts. These results support the proposed unsymmetrical binding and alkene polarization model.

(C) Symmetrical Alkene Adducts. The alkene NMR coordination shifts of **12a**,**j**,**k** are listed in Table 3. The C_{vinyl} and $C_{allylic}$ resonances exhibit quite small coordination shifts, while the H_{vinyl} and $H_{allylic}$ resonances show moderate downfield coordination shifts.[53] The vinyl $^1J_{CH}$ coupling constants of **12a**,**j**,**k** are unperturbed from the free alkene values.

(50) An alternative formulation of **12a**−**l** as insertion products with chelated ether ligands, i.e., $Cp'_2Zr(\kappa^2\text{-}C,O\text{-}CH_2CHRO^tBu)^+$ alkoxymetallocyclobutane complexes, can be safely rejected. Related neutral azametallocyclobutane complexes formed by alkene addition to Zr−imido species exhibit very large upfield coordination shifts for the "alkene" resonances, and much higher "metal−alkene" rotation barriers. Walsh, P. J.; Hollander, F. J.; Bergman, R. G. *Organometallics* **1993**, *12*, 3705.

(51) For stabilization of positive charge by a ferrocenyl substituent, see: (a) Ceccon, A.; Giacometti, G.; Venzo, A.; Paolucci, D.; Benozzi, D. *J. Organomet. Chem.* **1980**, *185*, 231. (b) Allenmark, S. *Tetrahedron Lett.* **1974**, *15*, 371. (c) Behrens, U. *J. Organomet. Chem.* **1979**, *182*, 89. (d) Prakash, G. K. S.; Buchholz, H.; Reddy, V. P.; de Meijere, A.; Olah, G. A. *J. Am. Chem. Soc.* **1992**, *114*, 1097. (e) Koch, E.-W.; Siehl, H.-U.; Hanack, M. *Tetrahedron Lett.* **1985**, *26*, 1493. (f) Siehl, H.-U.; Kaufmann, F.-P.; Apeloig, Y.; Braude, V.; Danovich, D.; Berndt, A.; Stamatis, N. *Angew. Chem., Int. Ed. Engl.* **1991**, *30*, 1479. (g) Kreindlin, A. Z.; Dolgushin, F. M.; Yanovsky, A. I.; Kerzina, Z. A.; Petrovskii, P. V.; Rybinskaya, M. I. *J. Organomet. Chem.* **2000**, *616*, 106. (h) Koridze, A. A.; Astakhova, N. M.; Petrovskii, P. V. *J. Organomet. Chem.* **1983**, *254*, 345.

Table 3. NMR Coordination Shifts ($\Delta\delta$) for Symmetrical Alkenes Coordinated to **6**[a]

cpd	alkene	C_{vinyl}	$C_{allylic}$	H_{vinyl}	$H_{allylic}$
12a	ethylene	−3.8	−	0.56	−
12j	*cis*-2-butene	0.2	3.7	0.99	0.40
12k	cyclopentene	1.8	1.7	0.78	0.34

[a] In CD_2Cl_2 at −89 °C; $\Delta\delta = \delta_{coord} - \delta_{free}$.

Table 4. Equilibrium Constants for Alkene Coordination to **6**[a]

cpd	alkene	K_{eq} (M^{-1})
12h	$H_2C{=}CHFc$[b]	4800(1100)
12f	$H_2C{=}CHO^tBu$	large[c]
12g	$H_2C{=}CHCH_2SiMe_3$	1700(400)
12a	$H_2C{=}CH_2$	7.0(6)
12i	$H_2C{=}C{=}CH_2$	6.7(3)
12b	$H_2C{=}CHMe$	5.4(2)
12c	$H_2C{=}CH^nBu$	4.8(8)
12d	η^2-1,5-hexadiene	3.7(1.1)
12j	*cis*-MeHC=CHMe	2.2(1)
12k	cyclopentene	2.1(1)
12e	$H_2C{=}CHCH_2{}^tBu$	1.9(1)
12l	$H_2C{=}CHCl$	≤0.1[d]
−	$H_2C{=}CH^tBu$	*x*[e]
−	$H_2C{=}CHSiMe_3$	*x*[e]
−	*trans*-MeHC=CHMe	*x*[e]
−	$H_2C{=}CHCH{=}CH_2$	*x*[e]
−	C_6H_6	*x*[e]
−	$H_2C{=}CMe_2$	poly[f]
−	$H_2C{=}CHPh$	poly[f]

[a] In CD_2Cl_2 solution, −89 °C; $K_{eq} = [Zr\text{-}L][\mathbf{6}]^{-1}[L]^{-1}$; L = alkene. [b] Fc = ferrocenyl. [c] Complete coordination observed. See text for details. [d] Adduct formation detected by line broadening of vinyl chloride ^{13}C NMR signals. [e] No complex formed; $K_{eq} \leq 0.1\ M^{-1}$. [f] Cationic polymerization rapidly occurs.

These data can be rationalized by the unsymmetrical coordination/alkene polarization model proposed above for monosubstituted alkene complexes, coupled with fast exchange of the two ends of the alkene, e.g. by rotation around the metal−(alkene centroid) axis. Under slow alkene rotation conditions, one alkene carbon resonance of an unsymmetrically bound symmetrical alkene would shift upfield, while the other would shift downfield, as observed for **12b**−**h**. Exchange of the two ends of the C=C bond would average these resonances, resulting in the small, net coordination shifts observed for **12a**,**j**,**k**. However, structurally characterized Ag^I−ethylene adducts, where back-bonding is minimal, contain symmetrically bound ethylene ligands.[26a−c]

Thermodynamics of Alkene Binding to 6. Equilibrium constants for alkene binding to **6** in eq 1, $K_{eq} = [\mathbf{12}][\mathbf{6}]^{-1}$-$[alkene]^{-1}$, were determined by ^1H NMR and are listed in Table 4.[54] The equilibria were studied directly for **12a**−**e**,**i**−**k**. Alkene complexes **12g**,**h** are formed quantitatively when 1 equiv of the substrate is added to **6**, and therefore K_{eq} values in these cases were determined by competition experiments with propyne and allyltrimethylsilane, respectively.

The coordination of ethylene to **6** to give **12a** was probed in detail. The equilibrium constant for ethylene coordination is $K_{eq} = 7.0(6)\ M^{-1}$ in CD_2Cl_2 at −89 °C. Under these conditions, at $[\mathbf{6}]_{initial} = 0.040\ M^{-1}$ and $[C_2H_4]_{initial} = 0.20\ M^{-1}$, ca. 55% of the total $Cp'_2Zr(O^tBu)^+$ exists as **12a**. This equilibrium constant is unchanged over the concentration ranges $[\mathbf{6}]_{initial} = 0.038$−$0.080\ M^{-1}$ and $[C_2H_4]_{initial} = 0.13$−$0.29\ M^{-1}$, consistent with the equilibrium shown in eq 1. Addition of $[Ph_3C][B(C_6F_5)_4]$ (2.4 equiv per total Zr) as an anion source does not affect K_{eq} at −89 °C. If **6** existed as the ion-pair structure **O** (Figure 3), addition of $B(C_6F_5)_4^-$ would shift the equilibrium in eq 1 to the left, since **12a** is unlikely to bind $B(C_6F_5)_4^-$.[55] In contrast, when PhCl (8 equiv per total Zr) is added to mixtures of **6** and ethylene at −89 °C in CD_2Cl_2, K_{eq} is decreased to $5.0(3)\ M^{-1}$, consistent with stronger binding of PhCl vs CD_2Cl_2 to **6**. This result supports the proposal that **6** exists as a solvent adduct in RCl solution (**P**, Figure 3) and that the equilibrium in eq 1 involves substitution of CD_2Cl_2 by alkene.

The data in Table 4 show how steric and electronic effects influence the binding of alkenes to **6**. Alkene binding strength varies in the order ethylene ≈ α-olefins > *cis*-alkenes > *trans*-alkenes (no coordination observed). There is only a small difference in the K_{eq} values for ethylene, propylene, and 1-hexene. α-Olefins are better σ-donors but are more sterically crowded than ethylene, and these effects compensate each other. However, more dramatic increases in the steric bulk of the alkene do inhibit binding; e.g. 4,4-dimethyl-1-pentene adduct **12e** is significantly less stable than ethylene adduct **12a**, and 3,3-dimethyl-1-butene (*tert*-butylethylene) and vinyltrimethylsilane do not bind to **6** at −89 °C. *cis*-Alkenes show decreased K_{eq} values due to increased steric crowding near the double bond, and *trans*-2-butene does not bind to **6**. The reason for the stronger binding of *cis*-2-butene vs that of *trans*-2-butene to **6** is unknown. The relative binding abilities of *cis*- and *trans*-alkenes are highly system-dependent.[11a,56]

Electron-donating groups on the alkene significantly enhance alkene coordination to **6**. *tert*-Butyl vinyl ether binds to **6** very strongly to give **12f**, in which the partial positive charge on C_{int} is stabilized by the O^tBu group (Figure 6). In fact, **12f** is stable without excess *tert*-butyl vinyl ether in solution between −89 and −69 °C in CD_2Cl_2. The K_{eq} value for *tert*-butyl ether coordination to **6** could not be determined but must be at least 600 times larger than that for the sterically similar alkene 4,4-dimethyl-1-pentene. However, the bound alkene in **12f** is displaced by PMe_3 to give $[Cp'_2Zr(O^tBu)(PMe_3)][B(C_6F_5)_4]$ (**13**) and free *tert*-butyl vinyl ether.

Vinylferrocene also binds strongly to **6** to form **12h**, despite the presence of the large ferrocenyl substituent close to the double bond. In fact, vinylferrocene binds almost 700 times more strongly to **6** than ethylene does. The partial positive charge at C_{int} in **12h** is stabilized by the ferrocenyl group (Figure 7).[51] Allyltrimethylsilane also binds strongly to **6** to form **12g**. The equilibrium constant for the allyltrimethylsilane coordination is 900 times larger than that for the sterically similar alkene 4,4-dimethyl-1-pentene. The partial positive charge on C_{int} in **12g** is stabilized by the β-Si group (Figure 8).[52]

(52) Lambert, J. B. *Tetrahedron* **1990**, *46*, 2677.
(53) Cyclopentene adduct **12k** exhibits only one $H_{allylic}$ resonance, whereas two resonances are expected if rotation around the metal−(alkene centroid) bond is fast. Most likely the two $H_{allylic}$ resonances overlap. However, it is also possible that the $H_{allylic}$ hydrogens are exchanged by nondissociative alkene face exchange. This process has been invoked to explain *trans*-1,3-enchainment in Zr-catalyzed cyclopentene polymerization. Kelly, W. M.; Wang, S.; Collins, S. *Macromolecules* **1997**, *30*, 3151.
(54) If the solvent term is included, the equilibrium expression for eq 1 is $K_{eq}' = K_{eq}[CD_2Cl_2]$ where K_{eq} is defined as in the text. If the solvent concentration is assumed to be independent of temperature, the value of $\Delta H°$ is not affected, but the entropy term becomes $\Delta S°' = \Delta S° + R\ \ln[CD_2Cl_2]$, where $R\ \ln[CD_2Cl_2] \approx 5.5$ eu.
(55) Control experiments confirmed that Ph_3C^+ does not interact with C_2H_4 or **6** under these conditions.
(56) (a) Liu, W.; Brookhart, M. *Organometallics* **2004**, *23*, 6099. (b) Muhs, M. A.; Weiss, F. T. *J. Am. Chem. Soc.* **1962**, *84*, 4697.

Table 5. Thermodynamic Data for Equilibria in eq 1 and Activation Parameters for Decomplexation (k_{-1}) for Ethylene and Propylene[a]

adduct	alkene	$\Delta H°$ (kcal/mol)	$\Delta S°$ (eu)	$\Delta H_{-1}^{\ddagger}$ (kcal/mol)	$\Delta S_{-1}^{\ddagger}$ (eu)	$\Delta G_{-1}^{\ddagger}$ (kcal/mol)[b]
12a	$H_2C{=}CH_2$	−3.6(1)	−16(4)	7.7(5)	−15(2)	11.2(1)
12b	$H_2C{=}CHMe$	−3.8(2)	−17(1)	8.1(9)	−12(4)	10.9(1)

[a] In CD_2Cl_2 solution. [b] At −39 °C.

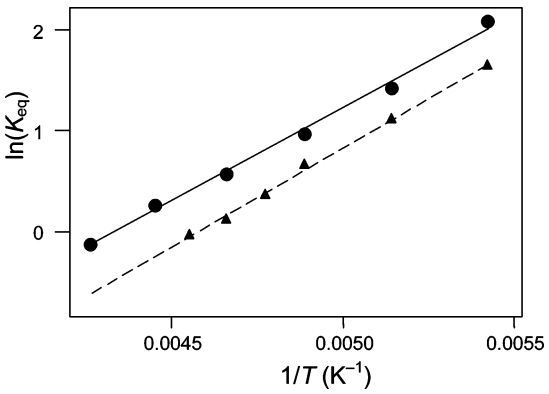

Figure 9. van't Hoff plot for ethylene (circles, solid line) and propylene (triangles, dashed line) coordination in **12a**,**b** in CD_2Cl_2 solution.

The presence of an electron-withdrawing group on the alkene inhibits alkene binding to **6**. When vinyl chloride is added to a solution of **6** in CD_2Cl_2 at −89 °C, the only evidence for coordination is selective line broadening of the vinyl chloride ^{13}C NMR signals, suggestive of minor formation of **12l** ($K_{eq} \leq 0.1\ M^{-1}$) and fast intermolecular exchange of free and bound vinyl chloride. An alternative formulation of **12l** as a Cl-bound halocarbon adduct cannot be ruled out. Vinyl chloride binds much more weakly than the sterically similar substrate propylene.

Enthalpy and Entropy of Ethylene and Propylene Coordination to 6. K_{eq} values for ethylene and propylene coordination to **6** were determined over a wide temperature range, enabling determination of binding enthalpies and entropies. These values are listed in Table 5. As the temperature is raised, formation of the alkene complexes **12a**,**b** become less favored and the equilibria shift to free alkene and **6**. Representative van't Hoff plots are given in Figure 9. The $\Delta H°$ and $\Delta S°$ values are both very similar for the two alkenes. The $\Delta S°$ values are modestly negative and would be less negative if a solvent term were included in the K_{eq} expression.[54]

Alkene Decomplexation. The NMR resonances of **12a**, **6**, and free ethylene in an equilibrium mixture in CD_2Cl_2 solution broaden as the temperature is raised above −89 °C. The Cp′ CH ^1H NMR signals of **12a** coalesce with those of **6** between −68 and −48 °C, and the coordinated ethylene signal coalesces with the free ethylene signal at ca. −30 °C. Study of this system in the fast exchange regime was difficult due to the lopsided equilibrium above −38 °C. These dynamic effects are consistent with the exchange of **12a** with **6** and of coordinated and free ethylene.

First-order rate constants for ethylene decomplexation from **12a** (k_{-1} in eq 1) were determined from the excess line broadening of the ethylene ^1H NMR signal of **12a** under slow exchange conditions. Ethylene decomplexation rates from **12a** are independent of the free ethylene concentration over the range $[C_2H_4] = 0.045{-}0.23\ M^{-1}$. Therefore, associative displacement

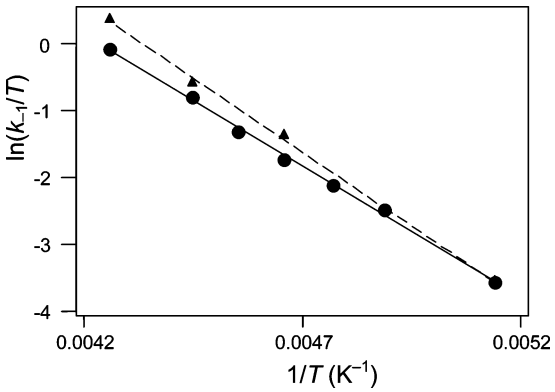

Figure 10. Eyring plot for ethylene (circles, solid line) and propylene (triangles, dashed line) decomplexation (k_{-1}) from **12a**,**b** in CD_2Cl_2 solution. The two rightmost data points for each line overlap.

of coordinated ethylene by free ethylene (eq 2) does not occur to a significant extent. Instead, the data imply that ethylene is lost from **12a** to give **6**, and ethylene coordinates to **6** to give **12a** (eq 1). An Eyring plot for ethylene decomplexation from **12a** is shown in Figure 10, and activation parameters for ethylene decomplexation are listed in Table 5.

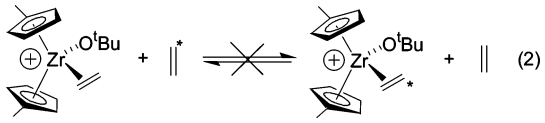

Similarly, when an equilibrium mixture of **12b**, **6**, and free propylene in CD_2Cl_2 is warmed above −89 °C, the NMR signals of **12b** broaden and eventually coalesce with those of **6** and free propylene. First-order rate constants were found by line shape analysis of the H_{int} resonance of **12b** using gNMR.[57] Propylene decomplexation rates are independent of the concentration of free propylene over the range $[C_3H_6] = 0.070{-}0.22$ M. Therefore, as for ethylene, free propylene does not directly displace coordinated propylene. The activation parameters for propylene decomplexation from **12b** (Figure 10 and Table 5) are very similar to those for ethylene decomplexation from **12a**.

The negative $\Delta S_{-1}^{\ddagger}$ values for ethylene and propylene decomplexation suggest that these reactions proceed by associative mechanisms in which the coordinated alkene is displaced by a CD_2Cl_2 molecule.

A free energy diagram that compares propylene and ethylene coordination to **6** at −39 °C is shown in Figure 11. It is clear that ethylene and propylene interact with the $Cp'_2Zr(O^tBu)^+$ cation in a nearly identical manner. The reason for this is that the steric and electronic differences between these two alkenes are small and exert compensating effects.

Electronic effects strongly influence the rate of alkene decomplexation and parallel the electronic effects on K_{eq}. Decomplexation of allyltrimethylsilane from **12f** is very slow, with $k_{-1} = 0.046(3)\ s^{-1}$ at −89 °C in CD_2Cl_2, as determined from a ^1H EXSY spectrum. In contrast, the rate constants for ethylene and propylene decomplexation under the same conditions are $k_{-1} = 1.5(1)$ and $2.3(1)\ s^{-1}$ respectively, as calculated from the corresponding activation parameters. The *tert*-butyl vinyl ether adduct **12f** also has a high decomplexation barrier.

(57) *gNMR*, v. 4.1.2; Adept Scientific: Letchworth, U.K., 2000.

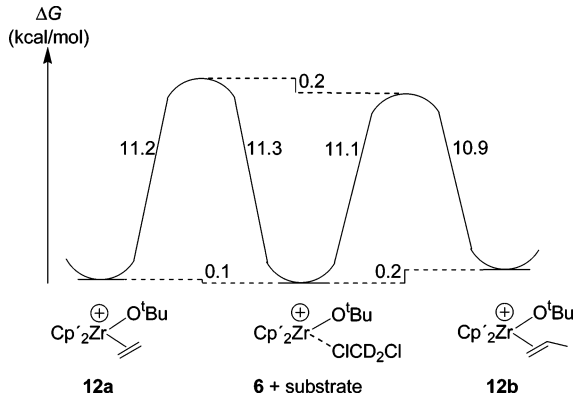

Figure 11. Free energy diagram (−39 °C) comparing ethylene and propylene coordination to **6** in CD_2Cl_2 solution.

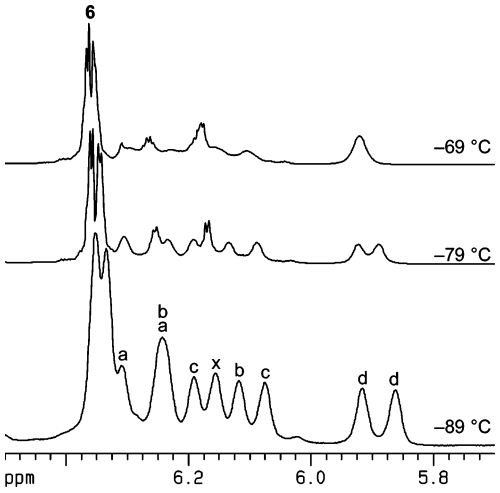

Figure 12. Variable-temperature ^{1}H NMR spectra of a mixture of **12f** and **6** in CD_2Cl_2 solution. The Cp′ CH region is shown. The sets of exchanging resonances of **12f** are labeled a−d and were established by EXSY spectroscopy. The large resonances at δ 6.36 labeled **6** are from **6**. The resonance at δ 6.18 labeled x is an unknown impurity.

Line broadening of the *tert*-butyl vinyl ether NMR resonances of **12f** is not observed up to −69 °C, and exchange between **12f** and **6** is not observed by EXSY spectroscopy at −89 °C. Moreover, no loss of **12f** is observed over 6 h at −89 °C in CD_2Cl_2. If decomplexation of *tert*-butyl vinyl ether from **12f** occurred, the free alkene would likely be cationically polymerized, resulting in net conversion of **12f** to **6**.

Dynamics of $Cp'_2Zr(O^tBu)(H_2C{=}CHO^tBu)^+$. The ^{1}H NMR Cp′ CH resonances of **12f** exhibit selective broadening between −89 and −69 °C and start to coalesce in a pairwise manner at −69 °C (Figure 12). A ^{1}H EXSY spectrum of **12f** (−89 °C) contains cross-peaks for pairwise exchange of the Cp′ CH resonances but does not show cross-peaks for exchange of **12f** with **6**. In addition, the ^{13}C NMR ipso-Cp′ and Cp′*Me* resonances of **12f** display line broadening at −79 °C. The Zr−O^{t}Bu and other alkene resonances of **12f** remain sharp between −89 and −69 °C. The resonances of **6** also remain sharp in this temperature range.

These results show that the two Cp′ rings of **12f** exchange with each other *without* decomplexation of the *tert*-butyl vinyl ether ligand and *without* exchange of the two sides of a given Cp′ ligand (site epimerization). The simplest exchange process that explains these results is nondissociative alkene face exchange, i.e. exchange of the $Cp'_2Zr(O^tBu)^+$ unit between the two enantiofaces of the alkene without decomplexation.

Table 6. NMR Coordination Shifts ($\Delta\delta$) for Vinyl Ethers and Sulfides[a]

cpd	substrate	C_{int}	C_{term}	H_{int}	H_{trans}	H_{cis}
14	$H_2C{=}CHOEt$	−5.4	14.3	−0.54	0.77	0.97
15	$H_2C{=}CHSMe$	−7.1	15.7	<0[b]	0.86	>0[b]

[a] In CD_2Cl_2 at −89 °C; $\Delta\delta = \delta_{coord} - \delta_{free}$. [b] The resonances for the coordinated substrate are obscured by Cp′ CH resonances, but the signs of the coordination shifts can be established because the H_{int} and H_{cis} resonances of free methyl vinyl sulfide are downfield and upfield of the entire Cp′ CH region, respectively.

Alkene enantioface exchange in **12f** probably proceeds by slippage of the alkene to an O-coordination mode (**12f′**), rotation around the O−C_{int} bond, and slippage back to the π-complex isomer (eq 3). This process is a functional-group-assisted olefin face exchange.[58] As noted below, ethyl vinyl ether, which is smaller than *tert*-butyl vinyl ether, forms a stable O-adduct with **6**.

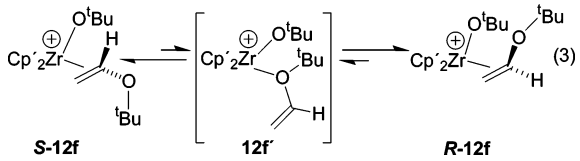

An alternative possible mechanism for alkene face exchange in **12f** is rotation around the C=C double bond, which may be weakened due to the $Cp'_2Zr(O^tBu)(H_2CC^+(H)O^tBu)$ carbocation-like resonance form (Figure 6). This kind of mechanism has been established for $CpFe(CO)_2(H_2C{=}CHNR_2)^+$ vinylamine complexes.[59] In addition to alkene face exchange, this mechanism results in exchange of H_{cis} with H_{trans} of the bound alkene. However, for **12f**, the H_{trans} and H_{cis} resonances are sharp between −89 and −69 °C, ruling out the C=C double bond rotation mechanism.

Vinyl Ether and Vinyl Sulfide Adducts. The reaction of **6** with ethyl vinyl ether or methyl vinyl sulfide yields the corresponding $[Cp'_2Zr(O^tBu)(\eta^1\text{-}RECH{=}CH_2)][B(C_6F_5)_4]$ adducts **14** (RE = EtO) and **15** (RE = MeS), as shown in eq 4. The NMR properties of **14** and **15** are very different from those of **12f** or the other monosubstituted alkene complexes **12b**−**e**,**g**,**h**. In particular, **14** and **15** display *upfield* coordination shifts for H_{int} and C_{int}, and *downfield* coordination shifts for C_{term} (Table 6), which are opposite in sign to those for **12b**−**h**. In addition, **14** and **15** display C_s symmetry at −89 °C instead of the C_1 symmetry observed for **12b**−**h**. These results show that the alkenes in **14** and **15** are coordinated by the heteroatom and not by the C=C bond. The putative O-bound *tert*-butyl vinyl ether adduct **12f′** in eq 4 is probably electronically favored over the C=C π-complex **12f** but is destabilized by steric crowding.

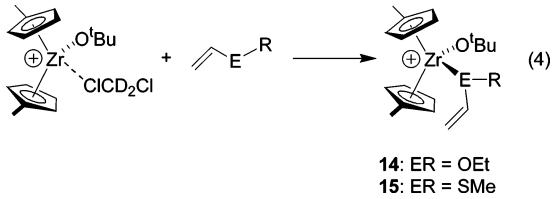

Diene Adducts. It might be expected that 1,3-butadiene would bind strongly to **6** in an η^2-fashion, as the positive charge

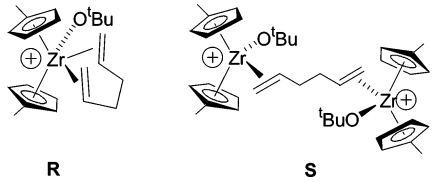

Figure 13. Unobserved 1,5-hexadiene coordination modes.

on C_{int} could be stabilized as an allyl-type cation.[60] However, 1,3-butadiene does not coordinate to **6**. The lack of 1,3-butadiene coordination may be due to conjugation. The conjugative stabilization of 1,3-butadiene is 3−4 kcal/mol,[61] while $\Delta H°$ of coordination for nonconjugated alkenes is ca. −3.7 kcal/mol (Table 5). Thus, if 1,3-butadiene were to lose conjugation upon η^2-coordination, perhaps due to rotation around the C_2-C_3 bond to minimize steric crowding, there likely would be no enthalpic advantage to coordination. Therefore, as $\Delta S°$ is expected to be negative, K_{eq} for 1,3-butadiene coordination would be extremely small. On the other hand, *chelated* η^2- and η^4-cyclopentadiene Zr^{IV} complexes are known.[13h,37b]

The NMR spectra of the 1,5-hexadiene adduct **12d** contain one set of strongly perturbed vinyl resonances and one set of only slightly shifted resonances, indicative of coordination of only one alkene unit. There is no evidence for formation of chelated bis-alkene complex **R** or dinuclear complex **S** (Figure 13).[60] The inability of 1,5-hexadiene to coordinate to two Zr centers to form **S** reflects the weakness of α-olefin coordination to **6**. Assuming that the K_{eq} value for formation of **S** from **6** and **12d** is the same as that for formation of **12d** from **6** and 1,5-hexadiene, under typical NMR conditions the concentration of **S** would be less than ca. 0.15 mM (<0.05[**12d**]), and therefore, this species would not be detectable by NMR. There is no evidence that the two ends of the 1,5-hexadiene ligand of **12d** undergo an associative intramolecular exchange process (i.e. with **R** as a transition state or intermediate).[62]

$Cp_2Zr(O^tBu)(H_2C{=}CHMe)^+$. The addition of excess propylene to **7** at −89 °C produces an equilibrium mixture of $[Cp_2Zr(O^tBu)(H_2C{=}CHMe)][B(C_6F_5)_4]$ (**16**), **7**, and free propylene, analogous to the formation of the Cp'_2Zr analogue **12b** in eq 1. The ^1H and ^{13}C NMR spectra of **16** each contain two Cp resonances, consistent with the expected C_1 symmetry. The NMR data for the bound propylene of **16** are very similar to the data for **12b**. The equilibrium constant for formation of **16**, $K_{eq} = [\mathbf{16}][\mathbf{7}]^{-1}[H_2C{=}CHMe]^{-1}$, is 14.7(7) M^{-1} (CD_2Cl_2, −89 °C), almost 3 times greater than that for formation of **12b** under the same conditions (eq 1). This difference is due to the greater Lewis acidity of **7** vs **6**, which results from the weaker electron-donating ability of Cp^- compared to that of Cp'^-.[63] Steric factors may also make a minor contribution to the difference in propylene binding strength in **16** vs **12b**.

Reactions of $Cp'_2Zr(O^tBu)^+$ with Other Potential Ligands. Neither N_2 (1 atm) nor H_2 (1 atm) displaces CD_2Cl_2 from **6** at −89 °C in CD_2Cl_2. N_2 and H_2 complexes of d^0 metals are as yet unknown.[64,65] Hydrogenolysis of Zr−alkyl bonds is thought to involve transient H_2 complexes.[66] Neither benzene nor in situ generated Ph_3CMe coordinate to **6** at −89 °C in CD_2Cl_2. Unfavorable steric interactions between the arenes and the *tert*-butoxide and Cp′ ligands may prevent coordination in this system. Arene complexes of d^0 metals are known in more sterically open systems.[67]

Discussion

NMR Properties and Structures of $Cp'_2Zr(O^tBu)(alkene)^+$ Species. The close similarity of the NMR data for nonchelated **12b**−**h** and structurally characterized chelates **A** and **B**[8] provides strong evidence that these species have similar unsymmetrical alkene binding modes. The lack of d−π* back-bonding and the shape of the alkene π-orbital allow the coordinated alkene to slide from a symmetrical to an unsymmetrical coordination mode to delocalize the positive charge from the metal to the alkene. For monosubstituted-alkene complexes **12b**−**h**, the slippage occurs such that the charge is delocalized primarily to C_{int}, which can stabilize the charge better than C_{term}, as secondary carbocations are more stable than primary carbocations. Incorporation of β-Si, α-OR, or α-metallocene functionalities in the alkene results in additional charge delocalization.

The NMR data for symmetrical-alkene complexes **12a**,**j**,**k** can be accommodated by the unsymmetrical binding model, with fast rotation around the metal−(alkene centroid) axis on the NMR time scale. However, the observed coordination shifts for symmetrical alkene complexes are small (Table 3) and are also consistent with symmetrical alkene binding, as has been established for Ag^I−ethylene adducts by X-ray crystallographic analysis.[26a−c]

The proposed unsymmetrical alkene binding in **12b**−**h** is supported by computational results. DFT calculations predict highly unsymmetrical propylene coordination (Δd(Zr−C) = 0.54 Å) in $\{H_2Si(C_5H_4)_2\}Zr(CH_3)(H_2C{=}CHMe)^+$, with the Zr−$C_{term}$ distance (2.57 Å) being significantly shorter than the Zr−C_{int} distance (3.11 Å).[68] Similar unsymmetrical propylene binding was predicted for the several possible propylene complexes in the *rac*-$Me_2C\{1\text{-}(3\text{-}^t\text{Bu-indenyl})_2\}Zr(CH_2CHMeEt)(H_2C{=}CHMe)^+$ system (Δd(Zr−C) = 0.27−0.73 Å).[69]

Interestingly, DFT calculations also predict unsymmetrical ethylene binding in $Cp_2Zr(CH_3)(C_2H_4)^+$ (Δd(Zr−C) = 0.22 Å) and $\{H_2Si(C_5H_4)_2\}Zr(CH_3)(C_2H_4)^+$ Δd(Zr−C) = 0.24 Å),[4a] in which the calculated Zr−C_{vinyl} lengths are similar to those in the calculated propylene adducts. Ab initio calculations predict unsymmetrical ethylene binding in $(C_5H_4SiH_2N^tBu)Ti(CH_3)$-

(58) The styrene complex $(C_5H_4CH_2CH_2N^iPr)V(=N^tBu)(H_2C{=}CHPh)^+$ undergoes a similar enantioface exchange by slippage to η-phenyl coordinated transient intermediates.[46]
(59) (a) Matchett, S. A.; Zhang, G.; Frattarelli, D. *Organometallics* **2004**, *23*, 5440. (b) Chang, T. C. T.; Foxman, B. M.; Rosenblum, M.; Stockman, C. *J. Am. Chem. Soc.* **1981**, *103*, 7361.
(60) The formation of $Cp'_2Zr(O^tBu)(\eta^4\text{-}H_2C{=}CHCH{=}CH_2)^+$ or $Cp'_2Zr(O^tBu)(alkene)_2^+$ species are probably precluded by O−Zr π-bonding.
(61) Wiberg, K. B.; Rosenberg, R. E.; Rablen, P. R. *J. Am. Chem. Soc.* **1991**, *113*, 2890.
(62) The pendant vinyl group of the 1,5-hexadiene may not be able to wrap around correctly to displace the bound vinyl group.
(63) Wieser, U.; Babushkin, D.; Brintzinger, H.-H. *Organometallics* **2002**, *21*, 920.
(64) MacKay, B. A.; Fryzuk, M. D. *Chem. Rev.* **2004**, *104*, 385.
(65) (a) Fryzuk, M. D.; Love, J. B.; Rettig, S. J.; Young, V. G. *Science* **1997**, *275*, 1445. (b) Basch, H. et al. *J. Am. Chem. Soc.* **1999**, *121*, 523.
(66) Gell, K. I.; Posin, B.; Schwartz, J.; Williams, G. M. *J. Am. Chem. Soc.* **1982**, *104*, 1846.
(67) (a) Hayes, P. G.; Piers, W. E.; Parvez, M. *J. Am. Chem. Soc.* **2003**, *125*, 5622. (b) Green, M. L. H.; Sassmannshausen, J. *Chem. Commun.* **1999**, 115. (c) Sassmannshausen, J. *Organometallics* **2000**, *19*, 482. (d) Gillis, D. J.; Quyoum, R.; Tudoret, M.-J.; Wang, Q.; Jeremic, D.; Roszak, A. W.; Baird, M. C. *Organometallics* **1996**, *15*, 3600. (e) Lancaster, S. J.; Robinson, O. B.; Bochmann, M.; Coles, S. J.; Hursthouse, M. B. *Organometallics* **1995**, *14*, 2456. (f) Jia, L.; Yang, X.; Stern, C. L.; Marks, T. J. *Organometallics* **1997**, *16*, 842.
(68) Schaper, F.; Geyer, M.; Brintzinger, H. H. *Organometallics* **2002**, *21*, 473.
(69) Moscardi, G.; Resconi, L.; Cavallo, L. *Organometallics* **2001**, *20*, 1918.

$(C_2H_4)^+$ (Δd(Ti−C) = 0.29 Å).[70] However, DFT computations predict more symmetrical ethylene binding in certain [$Cp_2ZrMe(C_2H_4)$][MAO] ion pairs (Δd(Zr−C) = 0.05−0.27 Å).[71] Further studies will be required to fully understand the coordination mode of symmetrical alkenes to $Cp_2Zr(X)^+$ species.

The NMR properties and proposed unsymmetrical alkene binding of d^0 complexes **12a**−**k** are significantly different from those of related d^2 metal−alkene complexes. For example, the Zr^{II}−butene complexes $Cp_2Zr(H_2C{=}CHEt)(THF\text{-}d_8)$ (**T**) and $Cp_2Zr(H_2C{=}CHEt)(PMe_3)$ (**U**) exhibit large *upfield* NMR coordination shifts for *both* alkene carbons ($\Delta\delta$ = ca. −75) and for the three vinyl protons $\Delta\delta$ = ca. −5.0), in sharp contrast to the coordination shifts of **12a**−**k** listed in Table 1.[72] The $^1J_{CH}$ values for the alkene unit of **U** (137−145 Hz) are significantly *decreased* from the values of free alkenes and **12a**−**k** (Table 2).[73] An X-ray crystallographic analysis shows that the butene ligand in **U** is coordinated symmetrically, with Δd(Zr−C) = 0.01(1) Å.[74] The chelated Zr^{II}−phosphine−alkene complexes $Cp''_2Zr(PPh_2CH_2CH_2CH{=}CH_2)$ (Cp″ = 1,2-$C_5H_3Me_2$) and $Cp_2Zr(PPh_2CH_2CH_2CH_2CH{=}CH_2)$ also exhibit symmetrical alkene binding (Δd(Zr−C) = 0.034(6), 0.058(4) Å).[75] The symmetrical coordination in these Zr^{II} systems provides good evidence that the unsymmetrical coordination proposed for **12b**−**h** and observed in **A** and **B** does not result from steric crowding or from chelation.

The Zr^{II}−ethylene complexes, $Cp_2Zr(H_2C{=}CH_2)(THF)$ and $Cp_2Zr(H_2C{=}CH_2)$(pyridine), exhibit large upfield alkene coordination shifts, low $^1J_{CH}$ values (140−145 Hz), and symmetrical ethylene binding (Δd(Zr−C) = 0.04(1) Å) in the solid state, similar to what is observed for $Zr^{II}(H_2C{=}CHR)$ adducts.[76] The upfield coordination shifts and symmetrical alkene binding in Zr^{II}−alkene complexes are caused by d−π* back-bonding in these d^2 complexes, and these species can be considered to be metallocyclopropanes. The alkene C=C distances in these complexes are lengthened by coordination to ca. 1.44 Å, consistent with metallocyclopropane formulation. In contrast, the absence of back-bonding in d^0 species results in divergent alkene NMR coordination shifts consistent with unsymmetrical alkene coordination.

Thermodynamics of Alkene Coordination to 6. Zirconium−alkene complexes **12a**−**l** exhibit weak metal−alkene binding. The $\Delta H°$ values show that the Zr−ethylene and Zr−propylene bonds are only ca. 3.7 kcal/mol stronger than the Zr−$ClCD_2Cl$ bond, which underscores the weakness of alkene coordination in these d^0 metal complexes. The weak binding is due to the lack of d−π* back-bonding. Consistent with a pure σ-donation binding mode, coordination is enhanced by the introduction of electron-donating groups in the alkene and by incorporation of functional groups to stabilize the positive charge buildup on C_{int}.

The metal−alkene interaction in **12a**−**l** is weaker than that in the chelates **A** and **B**.[8] Equilibrium mixtures of alkene adducts and solvent adducts are observed the for nonchelated systems, while **A** and **B** exist only as the alkene adduct even with the less weakly coordinating $MeB(C_6F_5)_3^-$ anion.[8a,b] This difference is expected due to the more favorable entropy of coordination in the chelated systems compared to that in nonchelated systems.

Alkene Exchange. Alkene adducts **12a**,**b** undergo reversible displacement of the alkene by CD_2Cl_2 solvent. Neither direct displacement of the coordinated alkene by free alkene nor displacement of the bound alkene by the $B(C_6F_5)_4^-$ anion is observed in **12a**,**b**. However, these processes may occur in less coordinating solvents.

Comparison of 12a−l with d^0 Metal−Alkene Complexes of Group 3, 5, and 6 Metals. The enthalpies of propylene binding in **12b** and $Cp^*_2Y(R)$(propylene) species **L** are similar.[17] However, **6** is stabilized by solvent coordination, Cp^*_2YR compounds are stabilized by agostic CH interactions,[17a] and the $Cp'_2Zr(O^tBu)^+$ unit is less crowded than the Cp^*_2YR units. Therefore, the alkene binding enthalpies of **12b** and **L** may not accurately reflect the relative strengths of Zr^{IV}−alkene and Y^{III}−alkene interactions. The K_{eq} for ethylene binding for Zr^{IV} (**12a**) in chlorobenzene is much smaller than that for ethylene binding to Nb^V (**J**; 220(10) M^{-1} at −30 °C in C_6D_5Cl), as **12a** does not form in this solvent.[15] Alkene binding in **12a**,**b** is also substantially weaker than alkene binding in V^V complex **I**, where adduct formation is even favorable at ambient temperature.[14,46] Additionally, cyclopentene binding in **12k** is much weaker than cycloheptene binding to W^{VI} in **K**.[16] A reasonable explanation for the stronger alkene binding in the groups 5 and 6 systems is that the V^V, Nb^V, and W^{VI} centers in **I**, **J**, and **K** are more electrophilic than the Zr^{IV} center in **12a**−**k**. Weak nonclassical back-bonding from M=NR, $M-NR_2$, or $M{=}CR_2$ bonding or nonbonding orbitals to the alkene π* orbital may also enhance alkene binding in the groups 5 and 6 systems.

Alkene decomplexation from **L** and related Y^{III} systems is much faster than for **12a**−**k**, which may reflect the fact that the displacing group is an incipient agostic C−H bond on the alkyl ligand in **L**.[17] Alkene decomplexation barriers for **I**, **J**, and **K** have not been reported. However, qualitative observations strongly suggest that decomplexation is slower than for **12a**−**l**,[14−16] which is consistent with stronger alkene coordination in the groups 5 and 6 systems.

NMR line broadening indicative of hindered metal−(alkene centroid) rotation is observed in the Nb^V and W^{VI} compounds **J** and **K**,[15,16] whereas in contrast, alkene rotation is fast on the NMR time scale for **12a**−**k** even at −89 °C. This difference may be due to the presence of nonclassical back-bonding in **J** and **K**, especially given the similar structures of the $Cp_2Nb(=N^tBu)^+$ and $Cp'_2Zr(O^tBu)^+$ cations. However, differences in metal−alkene distances may influence relative alkene rotation rates.

Comparison of 12a−l with Cp_2ZrR^+ Species and Implications for Polymerization. A $Cp_2Zr(OR)^+$ cation is a weaker Lewis acid than an analogous Cp_2ZrR^+ cation, due to O−Zr π-donation.[34d,77,78] This difference is reflected in the preferential binding of THF to Cp'_2ZrMe^+ vs **6** in competition experiments.[35] Therefore, it is expected that alkene coordination in **12a**−**l** and **16** is weaker than what would be expected in similar $Cp_2Zr(R)$(alkene)$^+$ species. However, the effects of alkene structure

(70) Lanza, G.; Fragalà, I. L.; Marks, T. J. *Organometallics* **2002**, *21*, 5594.
(71) Zurek, E.; Ziegler, T. *Faraday Discuss.* **2003**, *124*, 93.
(72) (a) Dioumaev, V. K.; Harrod, J. F. *Organometallics* **1997**, *16*, 1452. (b) Negishi, E.-i.; Holmes, S. J.; Tour, J. M.; Miller, J. A.; Cederbaum, F. E.; Swanson, D. R.; Takahashi, T. *J. Am. Chem. Soc.* **1989**, *111*, 3336.
(73) Binger, P.; Müller, P.; Benn, R.; Rufińska, A.; Gabor, B.; Krüger, C.; Betz, P. *Chem. Ber.* **1989**, *122*, 1035.
(74) Goddard, R.; Binger, P.; Hall, S. R.; Müller, P. *Acta Crystallogr., Sect. C* **1990**, *46*, 998.
(75) Yamazaki, A.; Nishihara, Y.; Nakajima, K.; Hara, R.; Takahashi, T. *Organometallics* **1999**, *18*, 3105.
(76) Fischer, R.; Walther, D.; Gebhardt, P.; Görls, H. *Organometallics* **2000**, *19*, 2532.

on alkene binding strength should be parallel for both Cp_2ZrR^+ and $Cp_2Zr(OR)^+$ cations.

Early transition metal catalysts are usually more active for ethylene polymerization than propylene polymerization (i.e. ethylene is consumed faster).[79a] Furthermore, ethylene/α-olefin copolymerization reactivity ratios show that ethylene is preferentially inserted vs the α-olefin into a $Cp_2Zr(copolymeryl)^+$ species, regardless of which monomer was previously inserted.[79b,80] Finally, ethylene inserts much faster into Y−H and Y−C bonds than propylene does.[17a] The present work shows that ethylene and propylene bind to **6** with approximately the same strength and exchange on and off with very similar rates in CD_2Cl_2 solution. These results suggest that the general lower activity for propylene polymerization compared to that for ethylene polymerization is not due to differential substrate binding but rather arises because propylene insertion (from the metal−alkene adduct) has a higher barrier than ethylene insertion. The larger size of propylene would lead to a more crowded insertion transition state and may explain this difference.

$(C_5R_5)_2ZrR^+$ polymerization catalysts typically have a strong preference for 1,2-insertion of α-olefins, i.e., the migrating Zr−*R* group migrates to C_{int}).[1b] The proposed unsymmetrical binding in **12b**−**h** and the resulting partial positive charge on C_{int} provide a simple explanation for this trend. The polarization should make C_{int} more susceptible to nucleophilic attack than C_{term}. Also, unfavorable steric interactions between the alkyl group of the α-olefin and the cyclopentadienyl ligands in $Cp_2Zr(R)(H_2C{=}CHR')^+$ species may favor the rotamer in which C_{int} is oriented toward the metal−alkyl bond, which may contribute to the preference for 1,2 insertion.

Experimental Section

General Procedures. All reactions were performed using glovebox or Schlenk techniques under a purified N_2 atmosphere, or on a high vacuum line. N_2 was purified by passage through columns of activated molecular sieves and Q-5 oxygen scavenger. CD_2Cl_2, C_6D_5Cl, and C_6H_5Cl were distilled from P_2O_5. C_6D_6 was distilled from Na/benzophenone. Benzene and hexanes were purified by passage though columns of activated alumina and BASF R3-11 oxygen removal catalyst. Cp'_2ZrMe_2 (**1**), Cp_2ZrMe_2 (**5**), and methyl vinyl sulfide were synthesized by literature procedures.[81] Other reagents were received from standard commercial sources. *tert*-Butyl alcohol was dried over K_2CO_3 and stored under vacuum or as a stock solution in benzene. $[Ph_3C][B(C_6F_5)_4]$, vinylferrocene, isobutene, ethylene, propylene, allene, 1,3-butadiene, propyne, *cis*-2-butene, *trans*-2-butene, hydrogen, and vinyl chloride were used as received. Cyclopentene, *tert*-butyl vinyl ether, ethyl vinyl ether, vinyltrimethylsilane, 1-hexene, 4,4-dimethyl-1-pentene, and allyltrimethylsilane were dried over CaH_2 before use. Styrene was degassed prior to use. PMe_3, 1,5-hexadiene, and 3,3-dimethyl-1-butene were dried over 3 Å molecular sieves prior to use.

Elemental analyses were performed by Midwest Microlab (Indianapolis, IN). ESI-MS experiments were performed with an HP Series 1100MSD instrument using direct injection via a syringe pump (ca. 10^{-3} M solutions). Good agreement between observed and calculated isotope patters was observed, and the listed *m*/*z* value corresponds to the most intense peak in the isotope pattern. NMR spectra were recorded on Bruker DRX 500 or 400 spectrometers in Teflon-valved NMR tubes at ambient probe temperature unless otherwise noted. ^1H and ^{13}C chemical shifts are reported relative to $SiMe_4$ and were referenced to the residual solvent signals. ^{19}F NMR spectra are reported and referenced relative to external $CFCl_3$. ^{11}B NMR spectra are referenced to external $BF_3{\cdot}OEt_2$. ^{31}P NMR spectra are reported to external 85% H_3PO_4 and are referenced to free PMe_3 (δ −61.0). NMR probe temperatures were calibrated by a MeOH thermometer.[82] Coupling constants are reported in Hz. Where ^{13}C-{gated−^1H} NMR spectra are reported, standard $^{13}C\{^1H\}$ NMR spectra were also recorded to assist in interpretation and assignment. For $H_2C{=}CHX$ substrates, H_{cis} is the H that is cis to H_{int}, and H_{trans} is the H that is trans to H_{int}.

NMR spectra of ionic compounds contain $B(C_6F_5)_4^-$ resonances at the free anion positions. ^{19}F NMR spectra were obtained for all compounds that contain this anion. Resonances for Ph_3CMe are present when cationic compounds are generated with Ph_3C^+ and used in situ. The data for $B(C_6F_5)_4^-$ and Ph_3CMe are given in the Supporting Information.

Generation of $Cp_2Zr(O^tBu)Me$ (4). An NMR tube was charged with Cp_2ZrMe_2 (13.4 mg, 0.0533 mmol), and C_6D_6 (0.69 mL) and *tert*-butyl alcohol (0.0770 mmol, 1.445 equiv) were added separately by vacuum transfer at −196 °C. The tube was warmed to 22 °C, shaken, and maintained at 22 °C for 30 min to afford a colorless solution. A ^1H NMR spectrum was obtained that established that **4** had formed quantitatively. The volatiles were removed under vacuum, C_6D_6 (0.65 mL) was added by vacuum transfer at −196 °C, the tube was warmed to 22 °C, and NMR spectra were recorded. This species was used in situ to prepare **7**. ^1H NMR (C_6D_6): δ 5.77 (s, 10H, Cp), 1.02 (s, 9H, O^tBu), 0.32 (s, 3H, ZrMe). $^{13}C\{^1H\}$ NMR (C_6D_6): δ 110.2 (Cp), 77.1 ($OCMe_3$), 31.8 ($OCMe_3$), 17.6 (ZrMe).

Synthesis of $[Cp'_2Zr(O^tBu)][B(C_6F_5)_4]$ (6). A flask was charged with Cp'_2ZrMe_2 (**1**, 1.1826 g, 4.231 mmol) and benzene (40 mL). The resulting solution was stirred at 22 °C, and *tert*-butyl alcohol (3.6 mL of a 2.1 M solution in benzene, 7.6 mmol, 1.8 equiv) was added by syringe. Gas evolution occurred. The colorless solution was stirred for 1.25 h, the volatiles were removed under vacuum, and the product was dried under vacuum for 22 h, giving a clear, colorless oil. A ^1H NMR spectrum confirmed that the oil was pure **2**.[31] **Data for 2:** ^1H NMR (C_6D_6): δ 5.69 (m, 2H, Cp′ CH), 5.65 (m, 4H, Cp′ CH), 5.51 (m, 2H, Cp′ CH), 2.01 (s, 6H, Cp′*Me*), 1.06 (s, 9H, O^tBu), 0.25 (s, 3H, ZrMe). ^1H NMR (C_6D_5Cl): δ 5.78−5.73 (m, 4H, Cp′ CH), 5.71 (m, 2H, Cp′ CH), 5.58 (m, 2H, Cp′ CH), 2.05 (s, 6H, Cp′*Me*), 1.07 (s, 9H, O^tBu), 0.13 (s, 3H, ZrMe). $^{13}C\{^1H\}$ NMR (C_6D_6): δ 121.7 (Cp′ ipso), 111.9 (Cp′ CH), 111.8 (Cp′ CH), 108.2 (Cp′ CH), 107.8 (Cp′ CH), 76.9 ($OCMe_3$), 32.1 ($OCMe_3$), 19.6 (ZrMe), 15.1 (Cp′*Me*). Compound **2** so obtained was dissolved in benzene (20 mL). A separate flask was charged with solid $[Ph_3C][B(C_6F_5)_4]$ (3.8030 g, 4.123 mmol, 0.98 equiv) and benzene (70 mL), giving a suspension of a yellow solid in a gold solution. The solution of **2** was added to the flask containing the $[Ph_3C][B(C_6F_5)_4]$ suspension. The mixture was stirred for 2.5 h at 30 °C to give a mixture of a dark oil and yellow supernatant. The supernatant was removed by cannula. The oil was washed with benzene (3 × 60

(77) For discussion of M−OR π-donation for early transition metals and lanthanides, see: (a) Steffey, B. D.; Fanwick, P. E.; Rothwell, I. P. *Polyhedron* **1990**, *9*, 963. (b) Coffindaffer, T. W.; Steffy, B. D.; Rothwell, I. P.; Folting, K.; Huffman, J. C.; Streib, W. E. *J. Am. Chem. Soc.* **1989**, *111*, 4742. (c) Kerschner, J. L.; Fanwick, P. E.; Rothwell, I. P.; Huffman, J. C. *Inorg. Chem.* **1989**, *28*, 780. (d) Caulton, K. G. *New. J. Chem.* **1994**, *18*, 25. (e) Howard, W. A.; Trnka, T. M.; Parkin, G. *Inorg. Chem.* **1995**, *34*, 5900. (f) Hillier, A. C.; Liu, S.-Y.; Sella, A.; Elsegood, M. R. J. *Inorg. Chem.* **2000**, *39*, 2635. (g) Petrie, M. A.; Olmstead, M. M.; Power, P. P. *J. Am. Chem. Soc.* **1991**, *113*, 8704. (h) Russo, M. R.; Kaltsoyannis, N.; Sella, A. *Chem. Commun.* **2002**, 2458. (i) Manz, T. A.; Fenwick, A. E.; Phomphari, K.; Rothwell, I. P.; Thomson, K. T. *J. Chem. Soc., Dalton Trans.* **2005**, 668.

(78) (a) Marsella, J. A.; Moloy, K. G.; Caulton, K. G. *J. Organomet. Chem.* **1980**, *201*, 389. (b) Britovsek, G. J. P.; Ugolotti, J.; White, A. J. P. *Organometallics* **2005**, *24*, 1685.

(79) (a) Möhring, P. C.; Coville, N. J. *J. Organomet. Chem.* **1994**, *479*, 1. (b) Kaminsky, W.; Arndt, M. *Adv. Polym. Sci.* **1997**, *127*, 143.

(80) For a recent example of preferential α-olefin incorporation vs ethylene, see: Irwin, L. J.; Reibenspies, J. H.; Miller, S. A. *J. Am. Chem. Soc.* **2004**, *126*, 16716.

(81) (a) Couturier, S.; Tainturier, G.; Gautheron, B. *J. Organomet. Chem.* **1980**, *195*, 291. (b) Samuel, E.; Rausch, M. D. *J. Am. Chem. Soc.* **1973**, *95*, 6263. (c) Doering, W. v. E.; Schreiber, K. C. *J. Am. Chem. Soc.* **1955**, *77*, 514.

(82) Van Geet, A. L. *Anal. Chem.* **1970**, *42*, 679.

mL); at each wash the supernatant was removed by cannula, leaving a yellow oil. The oil was then washed with hexanes (3 × 50 mL; 1 × 70 mL; 1 × 20 mL) yielding **6** (3.30 g, 80%) as a yellow solid.[83] The product was stored at −35 °C. **Data for 6:** ^{1}H NMR (C_6D_5Cl): δ 5.86 (m, 4H, Cp′ CH), 5.83 (m, 4H, Cp′ CH), 1.86 (s, 6H, Cp′*Me*), 1.02 (s, 9H, O^{t}Bu). ^{1}H NMR (C_6D_5Cl, −35 °C): δ 5.83 (m, 8H, Cp′ CH), 1.86 (s, 6H, Cp′*Me*), 1.02 (s, 9H, O^{t}Bu). ^{1}H NMR (CD_2Cl_2, −89 °C): δ 6.35 (br s, 4H, Cp′ CH), 6.33 (br s, 4H, Cp′ CH) 2.18 (s, 6H, Cp′*Me*), 1.22 (s, 9H, O^{t}Bu). ^{13}C{^{1}H} NMR (C_6D_5Cl): δ 129.2 (Cp′ ipso), 117.7 (Cp′ CH), 114.9 (Cp′ CH), 84.4 (O*C*Me$_3$), 31.3 (OC*Me$_3$*), 14.5 (Cp′*Me*). ^{13}C{^{1}H} NMR (C_6D_5Cl, −35 °C): δ 117.4 (Cp′ CH), 114.5 (Cp′ CH), 84.0 (O*C*Me$_3$), 31.0 (OC*Me$_3$*), 14.4 (Cp′*Me*). The ipso Cp′ peak is obscured by solvent. ^{13}C{^{1}H} NMR (CD_2Cl_2, −89 °C): δ 129.4 (ipso Cp′), 116.7 (Cp′ CH), 114.2 (Cp′ CH), 84.1 (O*C*Me$_3$), 30.9 (OC*Me$_3$*), 14.8 (Cp′*Me*). Anal. Calcd for $C_{40}H_{23}BOF_{20}Zr$: C, 47.97; H, 2.31. Found: C, 48.08; H, 2.51. ESI-MS (C_6D_5Cl/PhMe solution): Major cation observed: [Cp′$_2$Zr(O^{t}Bu)$^+$ − H] calcd *m*/*z* 320.1, found 320.0.

Generation of [Cp$_2$Zr(O^{t}Bu)][B(C$_6$F$_5$)$_4$] (7). A solution of Cp$_2$Zr(O^{t}Bu)Me (**4**, 0.0533 mmol) was prepared as described above, and the volatiles were removed under vacuum. Solid [Ph$_3$C][B(C$_6$F$_5$)$_4$] (49.3 mg, 0.0534 mmol) was added, and C_6D_5Cl (0.48 mL) was added by vacuum transfer at −196 °C. The tube was warmed to 22 °C and shaken, giving a deep yellow-orange solution. A ^{1}H NMR spectrum was obtained and showed that **7** had formed in 96% yield versus Ph$_3$CMe. ^{1}H NMR (C_6D_5Cl): δ 5.98 (s, 10H, Cp), 0.98 (s, 9H, O^{t}Bu). ^{1}H NMR (CD_2Cl_2, −89 °C): δ 6.50 (s, 10H, Cp), 1.19 (s, 9H, O^{t}Bu). ^{13}C{^{1}H} NMR (C_6D_5Cl): δ 116.0 (Cp), 85.0 (O*C*Me$_3$), 31.1 (OC*Me$_3$*). ^{13}C{gated−^{1}H} NMR (CD_2Cl_2, −89 °C): δ 115.5 (d, $^1J_{CH}$ = 177, Cp), 84.6 (s, O*C*Me$_3$), 30.5 (q, $^1J_{CH}$ = 126, OC*Me$_3$*).

Conversion of 7 to [{Cp$_2$Zr}$_2$(μ-OH)$_2$][B(C$_6$F$_5$)$_4$]$_2$ (8). The above NMR tube was maintained at 22 °C for 5 d, during which time yellow crystals separated from solution. A ^{1}H NMR spectrum revealed the complete disappearance of **7** and the formation of poly(isobutene) (54% based on Ph$_3$CMe) and unidentified metallocene products (total of 13% based on Ph$_3$CMe). An X-ray crystallographic analysis revealed the yellow crystals to be [{Cp$_2$Zr(μ-OH)}$_2$][B(C$_6$F$_5$)$_4$]$_2$.

General Procedure for Generation of [Cp′$_2$Zr(O^{t}Bu)(alkene)][B(C$_6$F$_5$)$_4$] (12a−l). An NMR tube was charged with **6** (25−50 mg), and CD_2Cl_2 (0.5−0.7 mL) was added by vacuum transfer at −78 °C. The tube was shaken at this temperature, giving a yellow solution. The tube was cooled to −196 °C, and the alkene (excess) was added by vacuum transfer. The tube was warmed to −78 °C and shaken, yielding a yellow solution. The tube was placed in an NMR probe that had been precooled to −89 °C. NMR spectra were obtained and showed that a mixture of **12a**−**l**, **6**, and free alkene was present. The detailed procedure and data for ethylene adduct **12a** are given below. Data for **12b**−**k**, and **13**−**16** are given in the Supporting Information.

Generation of [Cp′$_2$Zr(O^{t}Bu)(H$_2$C=CH$_2$)][B(C$_6$F$_5$)$_4$] (12a). An NMR tube was charged with **6** (26.8 mg, 0.0267 mmol), and CD_2Cl_2 (0.67 mL) was added by vacuum transfer at −78 °C. The tube was shaken at this temperature, giving a yellow solution. The tube was cooled to −196 °C, and ethylene (0.183 mmol) was added by vacuum transfer. The tube was warmed to −78 °C and shaken, yielding a yellow solution. The tube was placed in an NMR probe that had been precooled to −89 °C. NMR spectra were obtained and showed that a mixture of **12a** (0.022 M), **6** (0.018 M), and free ethylene (0.17 M) was present. Raising the temperature from −89 °C has the effect of decreasing the amount of **12a** in solution while increasing the amounts of **6** and free ethylene, and broadening the signals for **12a** and to a lesser extent those of **6** and free ethylene. The signals for **12a** eventually coalesce with those of **6** and free ethylene. **Data for 12a:** ^{1}H NMR (CD_2Cl_2, −89 °C): δ 6.35 (br m, 2H, Cp′ CH, overlaps with signal for **6**), 6.23 (br m, 4H, Cp′ CH), 6.11 (m, 2H, Cp′ CH), 5.92 (s, 4H, C_2H_4), 2.17 (s, 6H, Cp′*Me*), 1.22 (s, 9H, O^{t}Bu, overlaps with signal for **6**). ^{13}C{^{1}H} NMR (CD_2Cl_2, −89 °C): δ 127.1 (Cp′ ipso), 119.0 (t, $^1J_{CH}$ = 160, C_2H_4), 116.6 (Cp′ CH), 116.2 (Cp′ CH), 114.3 (Cp′ CH), 110.5 (Cp′ CH), 84.8 (O*C*Me$_3$), 30.7 (OC*Me$_3$*), 14.7 (Cp′*Me*).

X-ray Crystallographic Analysis of 8. Single crystals of **8** were obtained by the decomposition of **7** in C_6D_5Cl solution after 5 d. Crystallographic data are summarized in Table 7. Data were collected on a Bruker Smart Apex diffractometer using Mo Kα radiation (0.71073 Å). Repeated difference Fourier maps allowed recognition of all expected non-hydrogen atoms as well as a disordered C_6H_5Cl solvent molecule. The bridging atoms between Zr atoms were determined to be oxygen on the basis of bond lengths and thermal parameters. A weak peak about 0.8 Å from this oxygen was assigned to H to give an overall neutral charge. Final refinement was anisotropic for non-hydrogen atoms and isotropic for H atoms. The occupancy of the Cl atom of the solvent was refined to a value of 0.51 consistent with a disordered C_6H_5Cl solvent molecule. No anomalous bond lengths or thermal parameters were noted.

Table 7. Summary of X-ray Diffraction Data for **8**·C_6D_5Cl

formula	$C_{68}H_{22}B_2O_2F_{40}Zr_2{\cdot}C_6D_5Cl$
fw	1952.51
cryst syst	triclinic
space group	$P\bar{1}$
a (Å)	9.900(2)
b (Å)	12.250(3)
c (Å)	14.111(3)
α (deg)	89.956(4)
β (deg)	85.384(4)
γ (deg)	87.814(4)
V (Å^3)	1704.5(7)
Z	2
T (K)	100
cryst color, habit	pale yellow, rod
GOF on F^2	1.048
R indices ($I > 2\sigma(I)$)[a]	R1 = 0.0433
	*w*R2 = 0.1004
R indices (all data)[a]	R1 = 0.0533
	*w*R2 = 0.1041

[a] $R1 = \sum||F_o| - |F_c||/\sum|F_o|$; $wR2 = [\sum[w(F_o^2 - F_c^2)^2]/\sum[w(F_o^2)^2]]^{1/2}$, where $w = q/[\sigma^2(F_o^2) + (aP)^2 + bP]$.

Determination of Thermodynamic Parameters and Exchange Rates. (A) General Variable-Temperature NMR Procedure. NMR samples were prepared as described for **12a** above. The NMR tube was stored at −78 °C and placed in a precooled NMR probe. The probe was maintained at a given temperature for 20−30 min to allow the sample to reach thermal equilibrium, and then NMR experiments were conducted. When necessary, the temperature was raised 5 or 10 °C and the procedure repeated until the desired temperature range had been studied.

(B) Equilibrium Constant Measurements. Equilibrium constants, $K_{eq} = [\mathbf{12}][\mathbf{6}]^{-1}[\text{alkene}]^{-1}$, were determined by multiple (typically 2−4) ^{1}H NMR experiments in which $[\mathbf{6}]_{initial}$ and $[\text{alkene}]_{initial}$ were varied. For **12a**−**e**,**i**−**k**, K_{eq} values were determined by direct study of the equilibria in eq 1. For the equilibrium involving **12a**, relative amounts of **12a**, **6**, and free ethylene were determined from the integrations of the coordinated C_2H_4 resonance of **12a**, the Cp′*Me* resonance of **6** after the contribution from **12a** was subtracted, and the free C_2H_4 resonance, respectively. The number of moles of **12a** and **6** were determined by finding their respective mole fractions and multiplying by the original amount of **6** used. The number of moles of free ethylene was determined from the ratio of the integrations of free ethylene to **12a**. Concentrations were then determined by dividing the number of moles by the solution volume. K_{eq} values were found between −89 °C and −38 °C. The K_{eq} values for formation of **12b**−**e**,**i**−**k** were determined similarly; details are given in the Supporting Information.

The K_{eq} value for allyltrimethylsilane coordination in **12g** was determined by a competition experiment with free propyne and the

(83) One crop of **6** was contaminated with ca. 2% [Ph$_3$C][B(C$_6$F$_5$)$_4$]. Control experiments showed that this contaminant does not influence alkene coordination to **6**.

propyne adduct, $[Cp'_2Zr(O^tBu)(HC{\equiv}CMe)][B(C_6F_5)_4]$ (**17**).[27a] The equilibrium constant for the reaction:

$$\mathbf{17} + H_2C{=}CHCH_2SiMe_3 \leftrightarrows \mathbf{12g} + HC{\equiv}CMe$$

was defined to be $K_1 = [\mathbf{12g}][HC{\equiv}CMe][\mathbf{17}]^{-1}[H_2C{=}CHCH_2SiMe_3]^{-1}$. The relative amounts of **12g**, **17**, free allyltrimethylsilane, and free propyne were found from the $SiMe_3$ resonance of **12g**, the H_{term} resonance of **17**, the $SiMe_3$ resonance of free allyltrimethylsilane, and the methyl resonance of free propyne, respectively. The equilibrium constant for allyltrimethylsilane coordination to **6** is $K_{eq,\mathbf{12g}} = [\mathbf{12g}][\mathbf{6}]^{-1}[H_2C{=}CHCH_2SiMe_3]^{-1} = K_1{\cdot}K_{pro}$ where $K_{pro} = [\mathbf{17}][\mathbf{6}]^{-1}[HC{\equiv}CMe]^{-1}$.

The K_{eq} value for vinylferrocene coordination in **12h** was determined by a competition experiment with allyltrimethylsilane. The equilibrium constant for the reaction:

$$\mathbf{12g} + H_2C{=}CHFc \leftrightarrows \mathbf{12h} + H_2C{=}CHCH_2SiMe_3$$

was defined to be $K_2 = [\mathbf{12h}][H_2C{=}CHCH_2SiMe_3][\mathbf{12g}]^{-1}[H_2C{=}CHFc]^{-1}$. The relative amounts of **12h**, **12g**, free vinylferrocene, and free allyltrimethylsilane were found from the H_{int} resonance of **12h**, the H_{int} resonance of **12g**, the H_{trans} resonance of free vinylferrocene, and the $H_{allylic}$ resonance of free allyltrimethylsilane, respectively. The equilibrium constant for allyltrimethylsilane coordination to **6** is $K_{eq,\mathbf{12h}} = [\mathbf{12h}][\mathbf{6}]^{-1}[H_2C{=}CHFc]^{-1} = K_2{\cdot}K_{eq,\mathbf{12g}}$ where $K_{eq,\mathbf{12g}}$ is defined above.

Thermodynamic parameters ($\Delta H°$ and $\Delta S°$) were determined from van't Hoff plots of $\ln(K_{eq})$ versus $1/T$. Reported values for each case are the weighted average of results from at least three runs in which the initial concentrations of **6** and alkene were varied.[84]

(C) Exchange Rate Measurements. Variable-temperature ^1H NMR spectroscopy was used to determine the kinetics of ligand exchange for **12a** and **12b**. First-order rate constants for ethylene decomplexation from **12a** (k_{-1}) were determined by measuring the line width (in Hz) at half-height of the coordinated ethylene peak. The line width of the benzene peak (added as a line width standard) was used as the line width in absence of exchange for the coordinated ethylene resonance at each temperature. First-order rate constants were determined by the formula $k_{-1} = \pi(\omega - \omega_0)$, where ω is the line width at half-height of the coordinated ethylene peak and ω_0 is the line width at half-height of the benzene peak. All measurements were made in the slow-exchange region over the temperature range −89 to −39 °C.

First-order rate constants for propylene decomplexation from **12b** were determined by visually fitting simulated spectra to experimental spectra. Simulations were performed using gNMR.[57] The average line width of the trityl cation resonances was used as the line width in the absence of exchange of the coordinated propylene resonances at each temperature. The H_{int} resonance of coordinated propylene was simulated. Coupling constants of **12b** were determined directly, or when not possible, by using the coupling constants of free propylene. Coupling constants were assumed to be temperature independent. The gNMR program yields rates, which were converted to first-order rate constants by the formula: rate $= k_{-1}[\mathbf{12b}]$, where k_{-1} is the rate constant for propylene decomplexation from **12b**. All measurements were made in the slow-exchange region over a temperature range of −89 to −39 °C.

For **12a** and **12b**, first-order decomplexation rate constants k_{-1} were determined in at least three experiments with different initial concentrations of **6** and alkene. The k_{-1} values were found to be independent of the concentrations of **6**, of free alkene, and of **12**, consistent with the rate law rate $= k_{-1}[\mathbf{12}]$. Activation parameters for decomplexation were determined from Eyring plots of $\ln(k_{-1}/T)$ versus $1/T$. The reported values are the weighted averages of results from at least three runs.[84]

Acknowledgment. We thank the NSF (CHE-0212210) for financial support, the University of Chicago for a William Rainey Harper fellowship (E.J.S.), Dr. Ian Steele for determination of the crystal structure of **8**, and Drs. Orson Sydora and Chang-Jin Qin for the ESI-MS of **6**.

Supporting Information Available: Full citation for ref 65b; NMR data for free alkenes, **12b**−**k**, and **13**−**16**; additional experimental procedures; dynamics of allene complex **12i**, details of the crystal structure of **8** (pdf, cif). This material is available free of charge via the Internet at http://pubs.acs.org.

JA0575225

(84) The weighted average $\bar{x}$ is defined as $(\sum w_i x_i)/(\sum w_i)$ and the weighted standard deviation σ is defined by $\sigma^2 = \{\sum w_i(x_i - \bar{x})^2\}/\{\sum w_i\}$ where the weighing factors are $w_i = 1/\sigma_i^2$.